NASA CR66905

PLASMA REACTOR DEVELOPMENT FOR METHANE DECOMPOSITION TO ACETYLENE AND HYDROGEN

by Robert K. Ames

Prepared Under Contract No. NAS1-8254 by
THE BOEING COMPANY
Seattle, Washington

for Langley Research Center

NATIONAL AERONAUTICS AND SPACE ADMINISTRATION

ABSTRACT

Experimental apparatus was constructed to study high temperature decomposition of methane to acetylene and hydrogen. Data was obtained on Sabatier reactor performance, and anode designs were tested. Energy distributions in a plasma reactor were measured for various anode configurations and cathode-anode spacings. Conclusions were drawn on efficiencies of small hydrogen plasma reactors.

TABLE OF CONTENTS

LIST OF ILLUSTRATIONS

PLASMA REACTOR DEVELOPMENT FOR METHANE DECOMPOSITION TO ACETYLENE AND HYDROGEN

By Robert K. Ames

Biotechnology Department
Aerospace Group
The Boeing Company
NAS1-8254

1.0 INTRODUCTION

A majority of the oxygen recovery processes currently being developed produce, as a waste product, solid carbon which has proved difficult to handle and presents zero-gravity removal problems. One process, the Sabatier, results in methane (CH_4) as a waste product. If the methane is vented overboard, hydrogen (H_2) is lost, resulting in incomplete utilization of the available metabolic carbon dioxide (CO_2). If a hydrogen plasma reactor were developed for decomposing methane to acetylene (C_2H_2) and hydrogen, the oxygen recovery efficiency of the Sabatier process could be improved since the recovered hydrogen could be used to reduce additional metabolic carbon dioxide. A study was initiated by NASA-Langley Research Center under Contract NAS1-8254 to develop the design parameters for such a plasma reactor.

2.0 SUMMARY OF PROGRAM OBJECTIVES

The objective of the program was to conduct a study and test program leading to the eventual development of a plasma reactor in which methane from a Sabatier reactor is converted to acetylene and hydrogen. The expected results of this program were parametric and design data from which prototype hardware could be designed. Boeing's major tasks were:

1) Design, construct, and test a hydrogen plasma reactor to obtain data on stable plasma operating regimes over a range of hydrogen feed rates, d. c. power inputs and various geometric relationships of cathode and anode.

2) Design and construct a Sabatier reactor for reducing carbon dioxide to methane and water.

3) Select a specific plasma reactor configuration and using the methane feed from the Sabatier reactor, conduct tests to obtain parametric data on the conversion of methane to acetylene and hydrogen.

4) Performance test the plasma reactor configuration that gives the best methane conversion efficiency and minimum power requirements.

Item 4 was removed as a task during performance of the study.

3.0 SYSTEM DESCRIPTION

3.1 BASIC SABATIER

The basic Sabatier system shown schematically in Figure 3.1 is based on the reaction:

$$CO_2 + 4H_2 \longrightarrow CH_4 + 2H_2O$$

Hydrogen from an electrolytic cell is mixed with metabolic carbon dioxide and reacted to form methane and water. The water is separated and cycled back to the electrolytic cell along with make-up water. The electrolytic cell produces hydrogen for the Sabatier reaction and oxygen for use by the astronaut.

Assuming 100 percent reaction efficiency, 1.125 pounds of make-up water per man-day are required to meet the metabolic oxygen requirements of 2.0 pounds per man-day. Of the 2.25 pounds of carbon dioxide available per man-day, only 1.375 pounds are used by the system and the excess is purged to space. The methane produced by the Sabatier reaction is also purged to space.

3.2 EXTENDED SABATIER

The system studied during this contract combines the basic Sabatier system with a hydrogen plasma reactor and acetylene separator to form the "Extended" Sabatier System shown in Figure 3.2.

The plasma reactor accomplishes the conversion of methane to acetylene and hydrogen via the reaction: $2CH_4 \longrightarrow C_2H_2 + 3H_2$. The acetylene formed could be separated from the reactor exhaust by solid adsorbents such as molecular sieves, and either vented to space or stored for other uses. The hydrogen is recycled to the Sabatier reactor. Assuming 100 percent reaction efficiency, 0.46 pounds of make-up water per man-day are required to produce 2.045 pounds of oxygen per day when 100 percent of the available carbon dioxide is

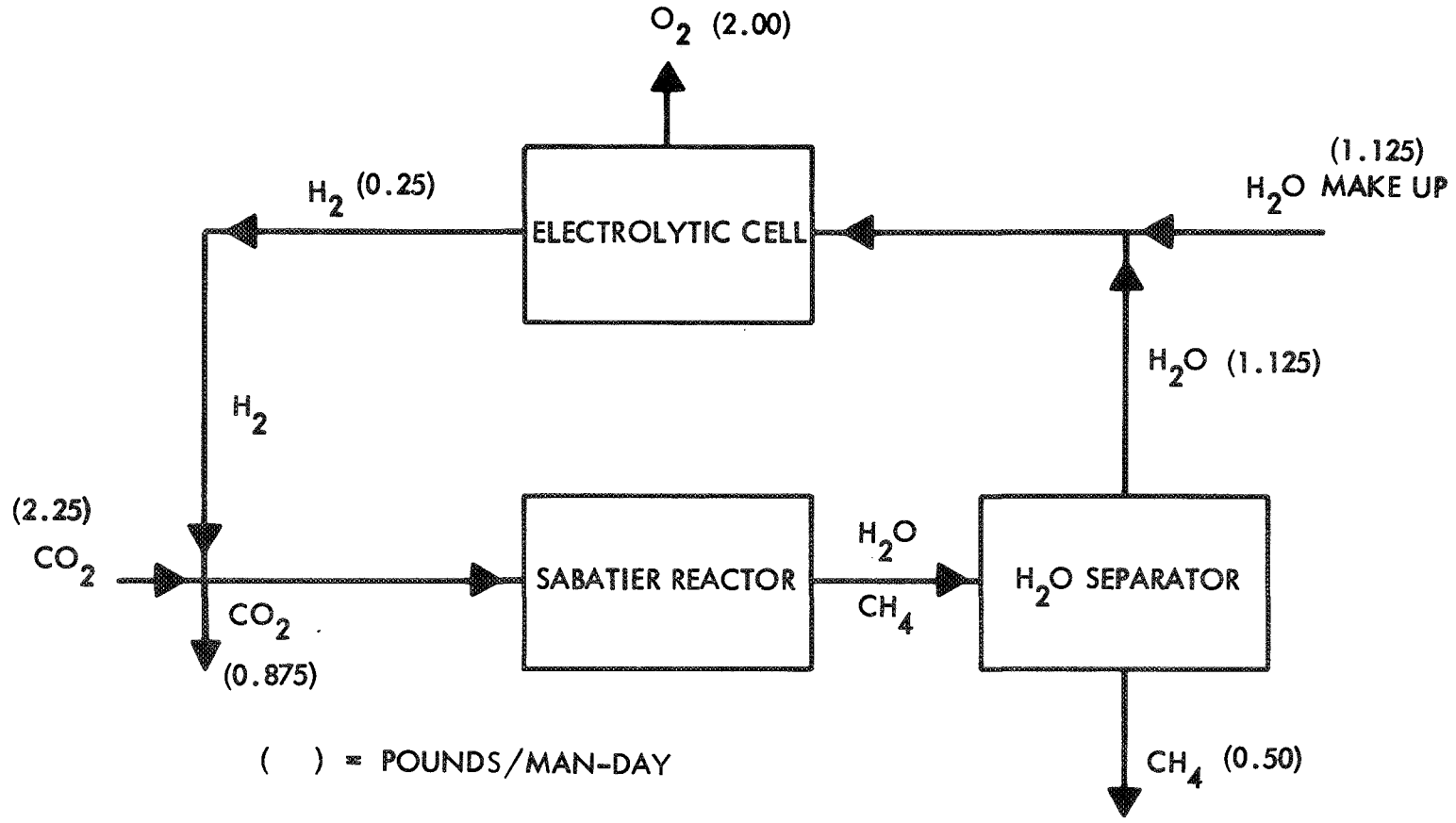

Figure 3.1: BASIC SABATIER SYSTEM

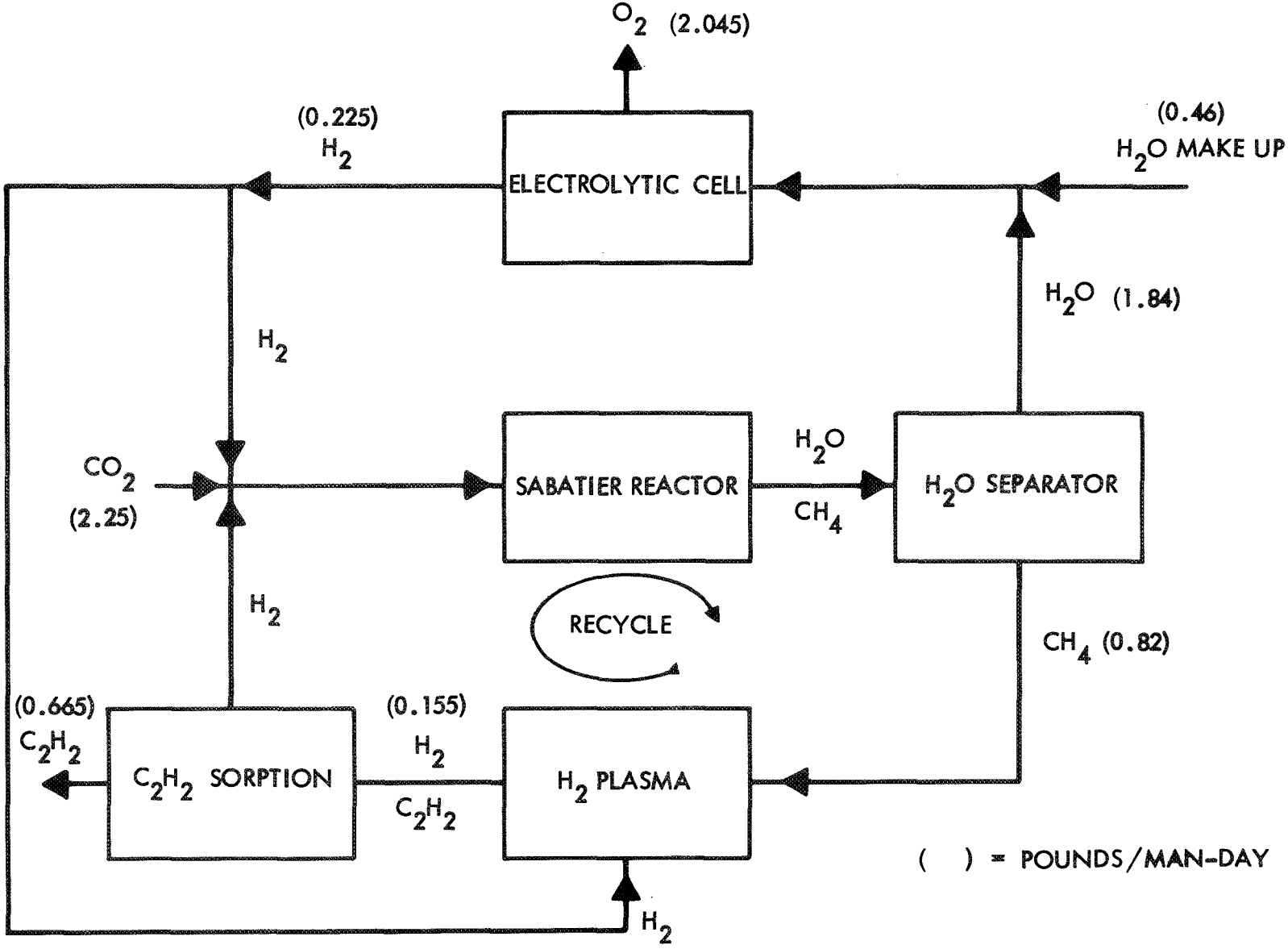

Figure 3.2: EXTENDED SABATIER SYSTEM

reacted. The methane reaction should approach 70 percent efficiency, thus necessitating a recycling of unreacted methane. The recycling of methane will provide approximately a 30% excess of hydrogen for the Sabatier reaction and essentially complete conversion of feed carbon dioxide. The 0.225 pounds per man-day hydrogen formed by the electrolytic cell is available as a feed to the plasma reactor or to the Sabatier reactor.

The utilization of the methane produced by the Sabatier reaction results in a reduction of water make-up of 0.665 pounds per man-day and better utilization of the metabolic carbon dioxide. Also, as with methane, the acetylene product, 0.665 pounds per man-day, is in a useable form for space station attitude control, or as a carbon source for food synthesis. Solid carbon formation is avoided as a potential system problem.

3.3 KINETICS

The thermal decomposition of methane is an extremely complex process which involves a number of stages producing various intermediate products. Ignoring the radical side reactions, the decomposition process is a series of successive stages during which methane is converted to ethane, ethane to ethylene, ethylene to acetylene, and acetylene to carbon and hydrogen. This is shown as:

$$CH_4 \xrightarrow{K_1} C_2H_6 \xrightarrow{K_2} C_2H_4 \xrightarrow{K_3} C_2H_2 \xrightarrow{K_4} C + H_2$$

The decomposition kinetics have been studied extensively and the results are shown graphically in Figure 3.3. The reaction rates of methane, ethane, and ethylene decomposition (K_1, K_2, K_3) are considerably faster than acetylene (K_4) at high temperatures, thus a high temperature reaction with appropriate reaction time and quenching can "freeze" the reaction at the acetylene step, minimizing the formation of carbon. Figure 3.4 represents the dependence of methane conversion on reaction temperature and a resulting reaction time. Conversion of 70 to 80 percent of methane can be expected at approximately 2100°K and 0.2 milliseconds reaction time.

4.0 PLASMA REACTOR DESIGN

An assembly drawing of the plasma reactor used in the test program is shown in Figure 4.1 and an artist's conceptual cut-away is shown in Figure 4.2. The basic arc heater design provided by Electro-Optical systems was used and extended to provide the methane reaction and quench zone downstream of the

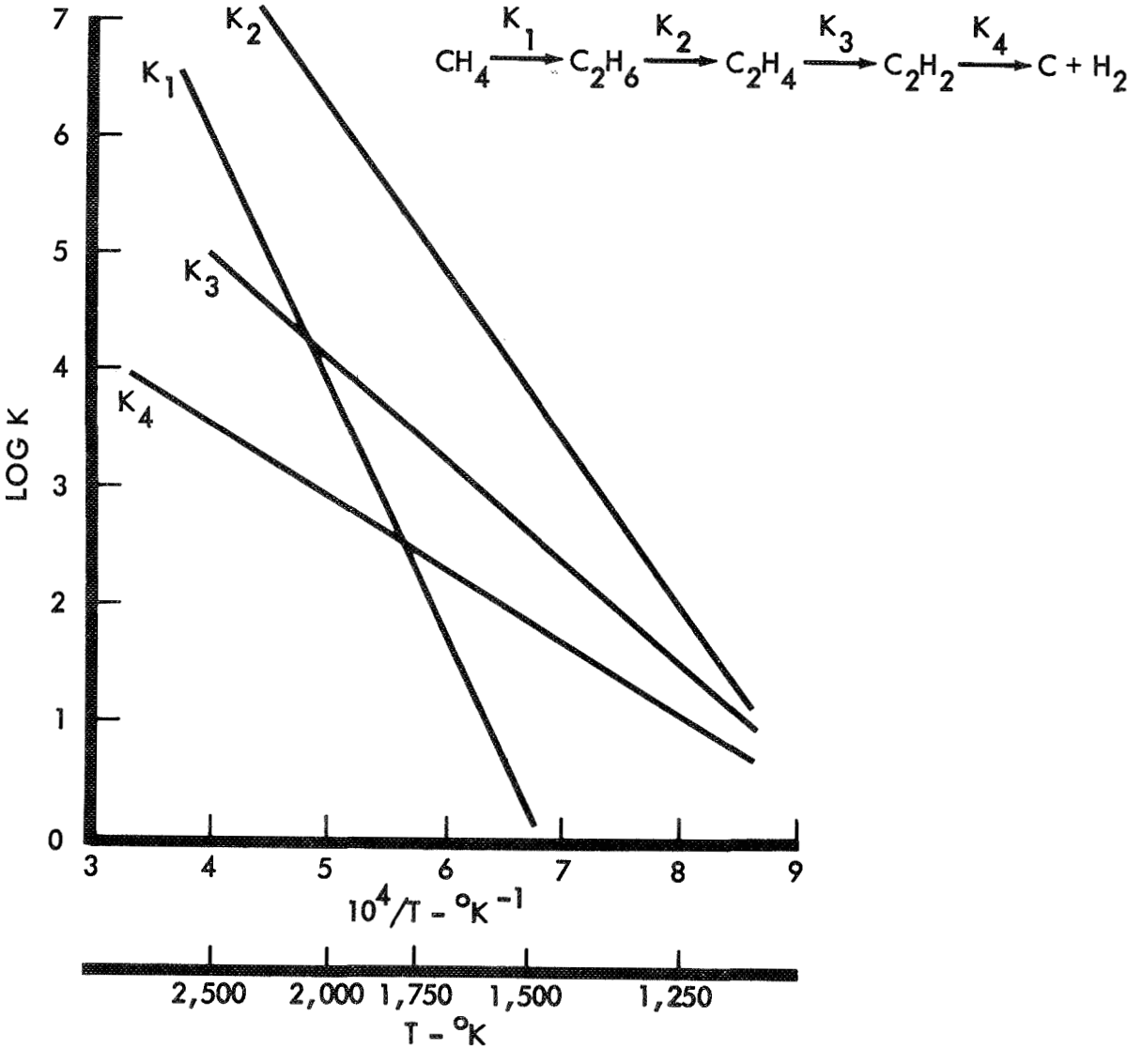

Figure 3.3: REACTION RATE CONSTANT VERSUS TEMPERATURE

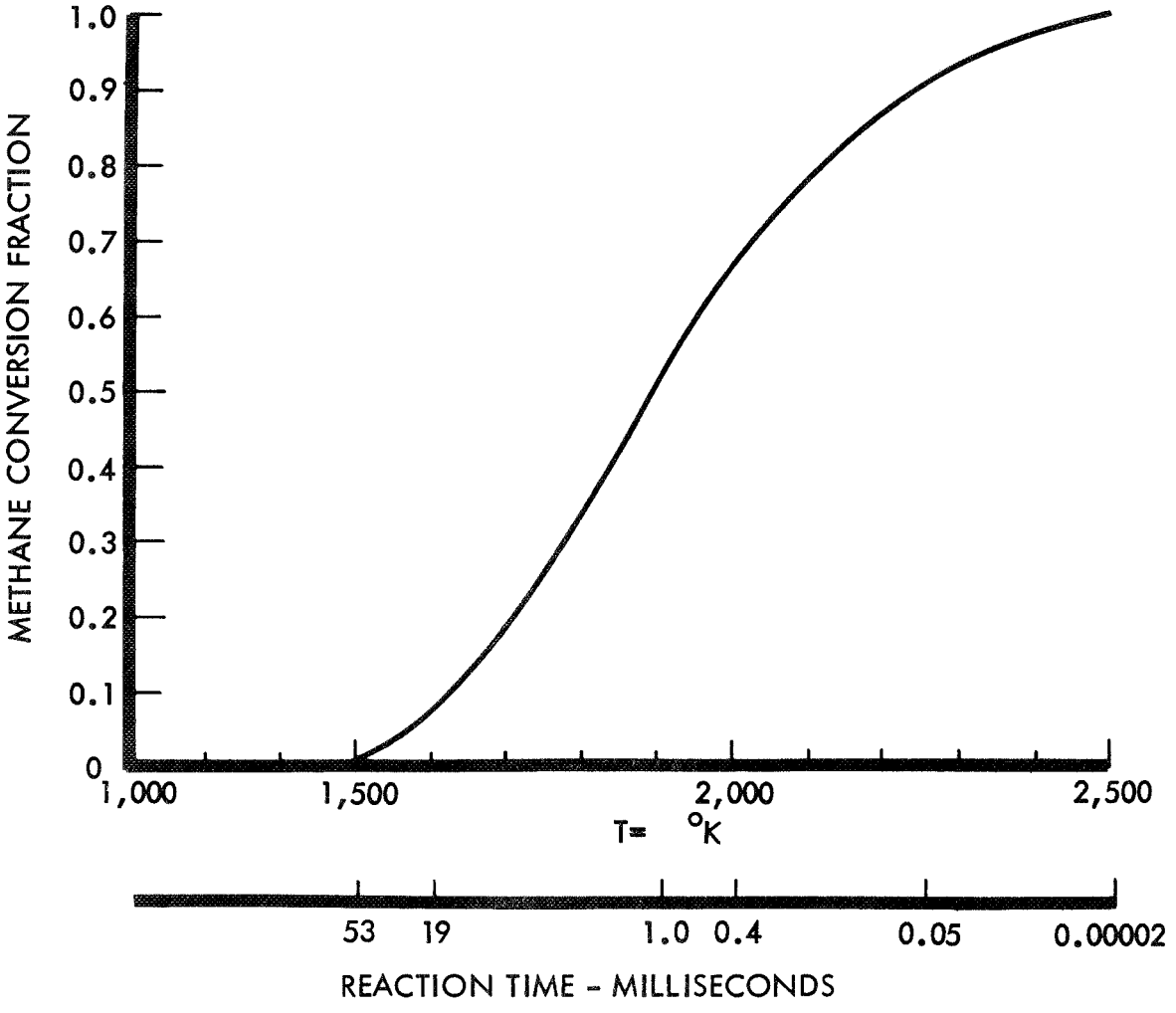

Figure 3.4: METHANE CONVERSION TO ACETYLENE VERSUS TEMPERATURE AND REACTION TIME

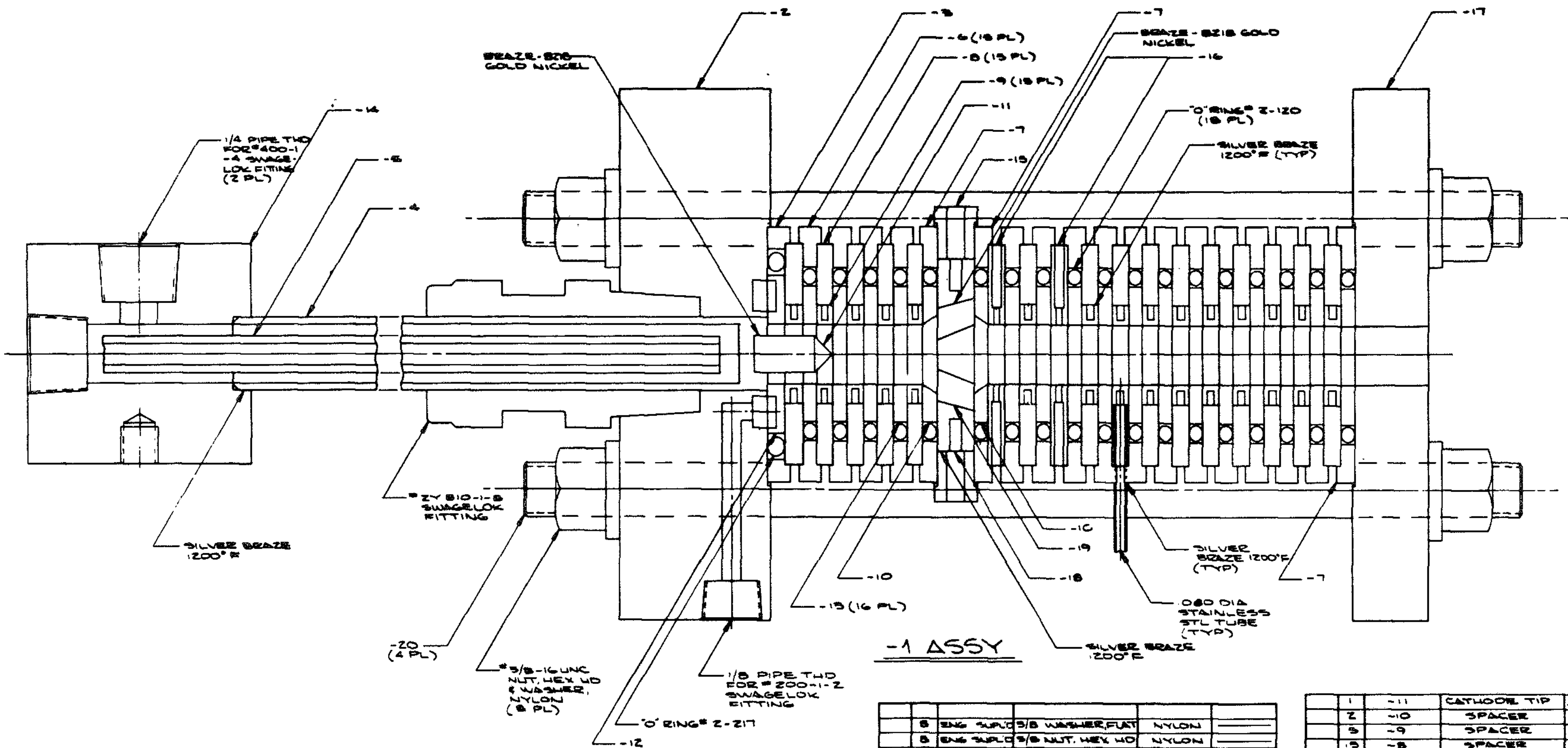

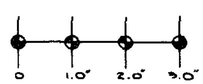

	8	ENG SUPL'D	5/8 WASHER, FLAT	NYLON	——
	8	ENG SUPL'D	5/8 NUT, HEX HD	NYLON	——
	1	2-217	"O" RING	HIGH TEMP SILICONE	——
	16	2-120	"O" RING	HIGH TEMP SILICONE	——
	1	ZY810-1-8	SWAGELOK FIT.	——	——
	2	400-1-4	SWAGELOK FIT	——	——
	1	200-1-2	SWAGELOK FIT.	——	——
	4	-20	SHAFT	NYLON	5/8 D x 6 3/4
	1	-19	ANODE	2% TH TUNGSTEN	3/8 x 7/8 D
	1	-18	INSERT	COPPER	3/8 x 1 5/8 D
	1	-17	END PLATE	COPPER	5/8 x 3 3/4 D
	2	-16	SPACER	COPPER	1/8 x 1 7/8 D
	1	-15	PLATE, ANODE	COPPER	3/8 x 2 1/8 D
	1	-14	ASSY, CATHODE	COPPER	1 3/4 x 1 3/4 D
	16	-13	SPACER	BORON NITRIDE	1/8 x 1 D
	1	-12	GAS RING	BORON NITRIDE	7/16 x 1 1/8 D

	1	-11	CATHODE TIP	2% TH TUNGSTEN	1/4 D x 3/8
	2	-10	SPACER	BORON NITRIDE	1/8 x 1 D
	3	-9	SPACER	COPPER	7/16 x 3/4 D
	15	-8	SPACER	COPPER	1/8 x 1/2 D
	3	-7	SPACER	PHENOLIC G-10	5/16 x 2 D
	16	-6	SPACER, "T" RING	PHENOLIC G-10	5/16 x 2 D
	1	-5	TUBE, INNER	STN STL	1/4 D x 4 1/2
	1	-4	TUBE, OUTER	COPPER	3/4 D x 3 1/2
	1	-3	SPACER	PHENOLIC G-10	5/16 x 2 D
	1	-2	PLATE	COPPER	1/4 x 3 3/4 D
	1	-1	ASSY	——	——

.010
30'

32✓

x G. BOWEN 8/68

x R K Ames 8/68

ASSY- PLASMA REACTOR

3/1 x NAS1-8254 29-43096 1/2

Figure 4.1: PLASMA REACTOR ASSEMBLY

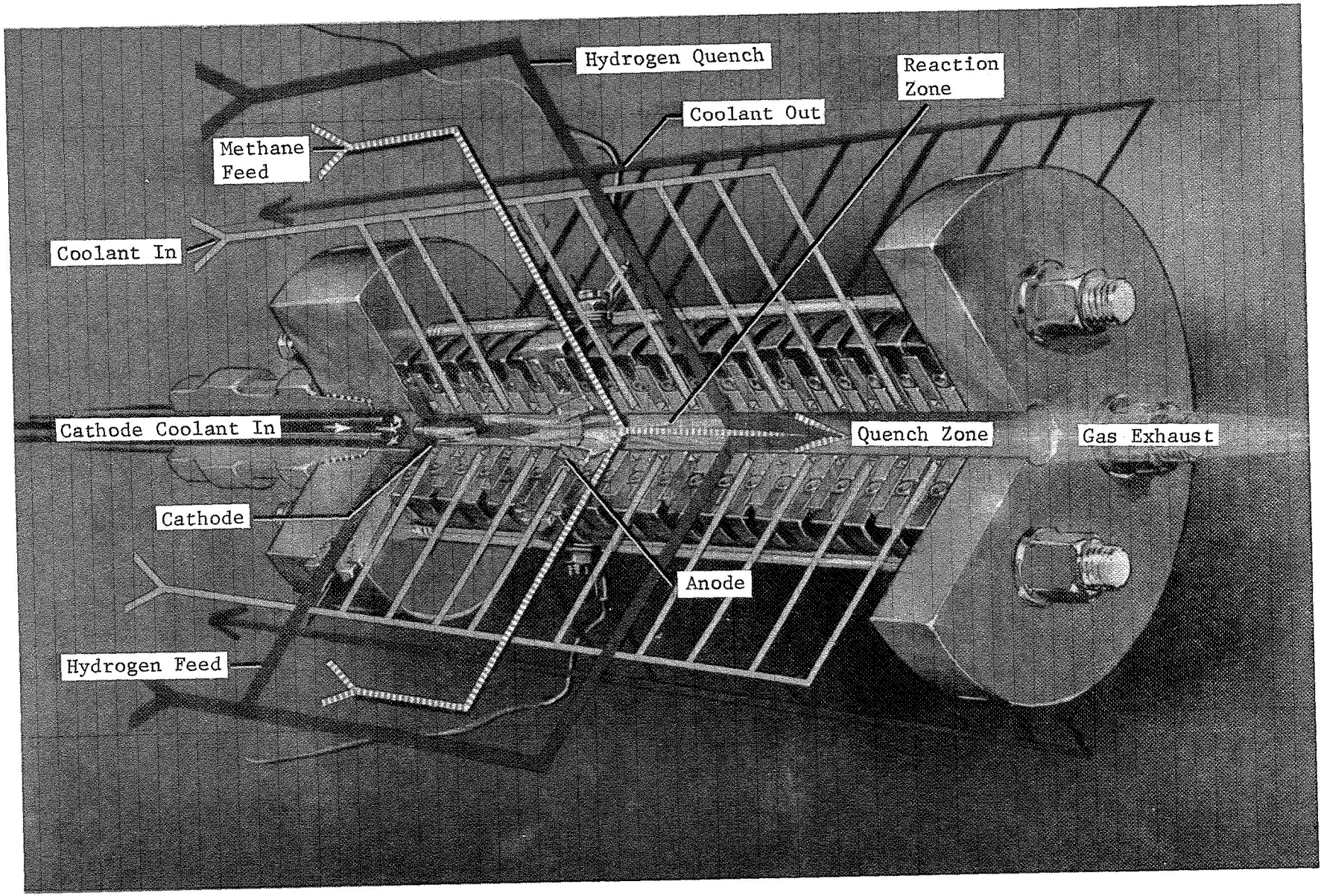

Figure 4.2: PLASMA REACTOR

anode (part - 19). A methane feed spacer was placed just downstream of the anode, and the hydrogen quench feed was adjustable at multiples of 0.2 inches downstream of the methane feed.

For the operation of the plasma reactor a hydrogen mass flow rate of 0.20 and 0.45 lb/day were projected for the four and nine man configurations respectively. These flow rates are equivalent to 1.059×10^{-3} and 2.3646×10^{-3} g/sec. In order for the desired reaction to take place in the reactor and proceed in the correct direction, the total enthalpy of the hydrogen before entering the reaction zone has to be 275×10^{3} BTU/lb-mole hydrogen (0.3169×10^{6} joules/g).[1] The total energy required to raise the hydrogen to the desired energy level is $P_{Gas} = \Delta H \times \dot{W}$ where:

$\dot{W}$ = mass flow rate, g/sec

ΔH = total enthalpy increase, joules/g

P_{Gas} = total power in the gas, joules/sec or watt

For the two flows under consideration, the gas power is therefore P_{Gas} = 333 watts and 750 watts respectively.

The electric power required for the heating of the gas is a function of the overall efficiency of the arc heater. The predominant losses in the heater are due to radiation from the arc and to convective heat transfer to the confinements of the heater. These losses are determined by the operating conditions of the arc with respect to arc current and arc voltage. The higher the arc current, the higher will be the losses due to radiation. On the other hand, if the arc voltage is relatively high the convective losses will predominate.

In addition, the inherent losses due to the anode voltage drop and the cathode voltage drop have to be considered. These two losses are also a function of the arc current. Because of the interrelation between efficiency and operating condition and the operating condition being determined by the overall efficiency, the total actual electric power requirements have to be found by a trial and error solution.

---

[1] An Analytical Approach to Plasma Torch Chemistry, J. E. Anderson and L. K. Case, Ind. and Eng. Chem. Process Design and Development, Vol. I, No. 3, 1962, pgs 161-165.

For a first cut at the design of the arc heater, an arc efficiency of 30 percent was assumed. This efficiency considers only the efficiency of the arc column, i.e.,

$$\eta = P_{Gas}/P_A$$

Where

$$P_A = V_A \times I_A$$

η = efficiency
P_A = power of arc
V_A = arc voltage
I_A = arc current

For the two configurations under consideration, the arc power was projected at P_A = 1110 watts and 2498 watts respectively. The arc voltage and are current relations for these two power levels are shown in Figure 4.3. In order to estimate the current level at which the heater can be operated, an estimate of the ionization level of the gas was made. The results indicated that the amount of gas ionized is still very low despite the high temperature of the gas and that the plasma must be operated at a relatively high arc current for the power levels expected. Based on Electro-Optical, Inc. experience, an arc current of I_A = 40 amps was selected.

For the four man configuration, the arc voltage was estimated V_A = 27.8 volts. The total voltage with which the arc heater should operate is the sum of the arc voltage and the voltage drops across the electrodes. The anode voltage drop should be approximately ϕ_A = 14 volts while the cathode voltage drop should be ϕ_C = 4 to 6 volts. A total voltage drop of 20 volts was assumed for the electrodes. The total projected operating voltage was estimated as V_T = 48 volts.

From Figure 4.4 the voltage gradient for a 40 amp arc operating with hydrogen is found to be E = 35 volts/cm. The distance between the anode and the cathode was calculated to be

$$d_E = 27.8/35 = 0.794 \text{ cm}$$
$$= 0.31 \text{ inches}$$

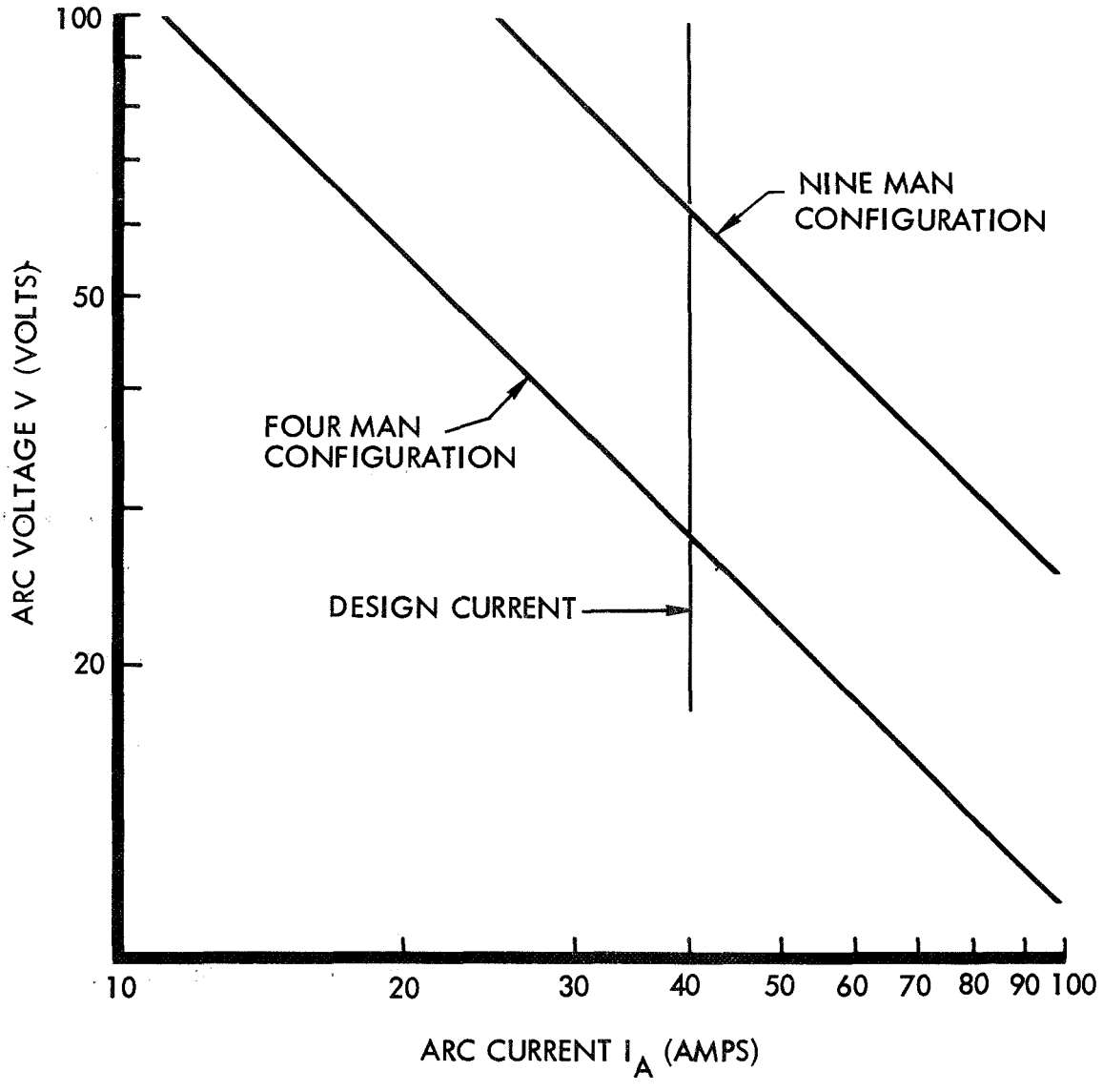

Figure 4.3: HYDROGEN ARC CURRENT - VOLTAGE RELATIONS

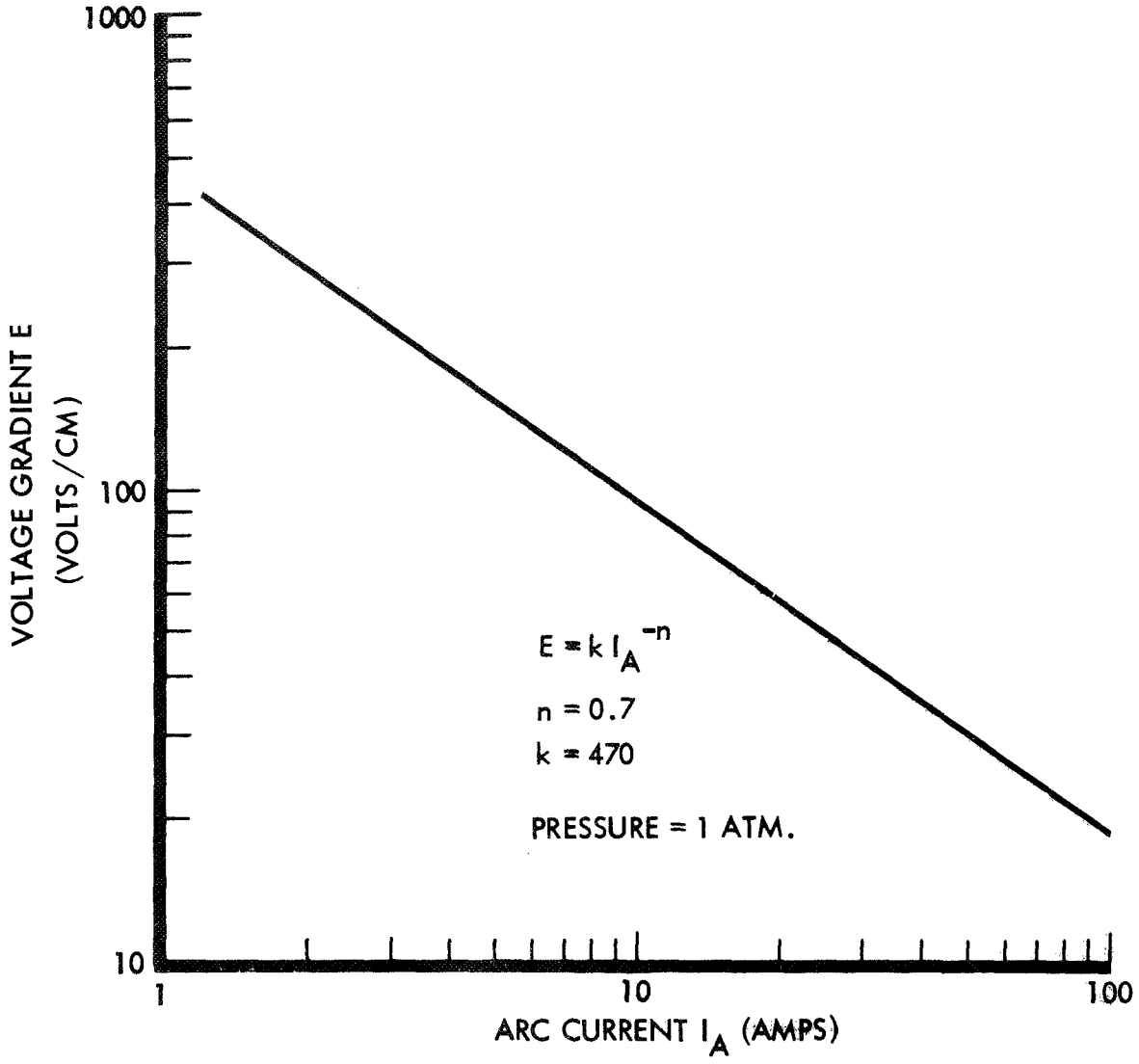

Figure 4.4: HYDROGEN VOLTAGE GRADIENT

Based on similar consideration, the distance between the cathode and the anode was found to be d_E = 1.771 cm or 0.697 inches for the nine man arc heater configuration. This is the setting shown in the plasma reactor assembly drawing in Figure 4.1 In Figure 4.5 the total voltage-arc current characteristics for the two arc heater configurations are shown. It can be seen that in both cases the arc will operate with a fairly steep negative slope. In order to maintain the arc, the voltage-current characteristics of the power supply with which the heater is operated will need a slope at least as steep as the arc. If the slope of the power supply does not satisfy the slope requirement, then the characteristic of the supply has to be improved by ballast resistance in series with the arc. The design of an arc heater for the plasma reactor was evaluated for the two mass flow rates under consideration. The results indicated that the total electric power requirement, P_T, for the two configurations should be approximately 1920 and 3280 watts for the four and nine man configuration respectively, assuming η equals 30 percent.

Considerations based on the arc current-total voltage relations have indicated that for each of the two mass flow rates a rather specific arc heater configuration with respect to electrode separation is required. It is clearly indicated that the desired energy elevel at one flow rate can not be reached using the same geometric configuration at a substantially different flow rate. The arc heater design must therefore allow for adjustments in the configuration according to the desired operating conditions. As seen in the assembly drawing (Figure 4.1) an infinite adjustment of cathode-anode spacings is available by either moving the cathode in the swage lock fitting and/or adding or removing constrictor spacers between the cathode and anode.

5.0 SABATIER REACTOR DESIGN

The Sabatier reactor, Figure 5.1, consists of a one-inch stainless steel tube combined integrally with a surrounding one and one-quarter inch stainless steel tube held in place by heat exchange fins. One end is capped with a standard flared-tube plug modified to contain an electric heater cartridge. A catalyst retainer is fitted at the outlet end of the reactor, limiting the catalyst charge from plugging the outlet.

The reactant feed gases enter the reactor via the flared tube fitting at the 90°

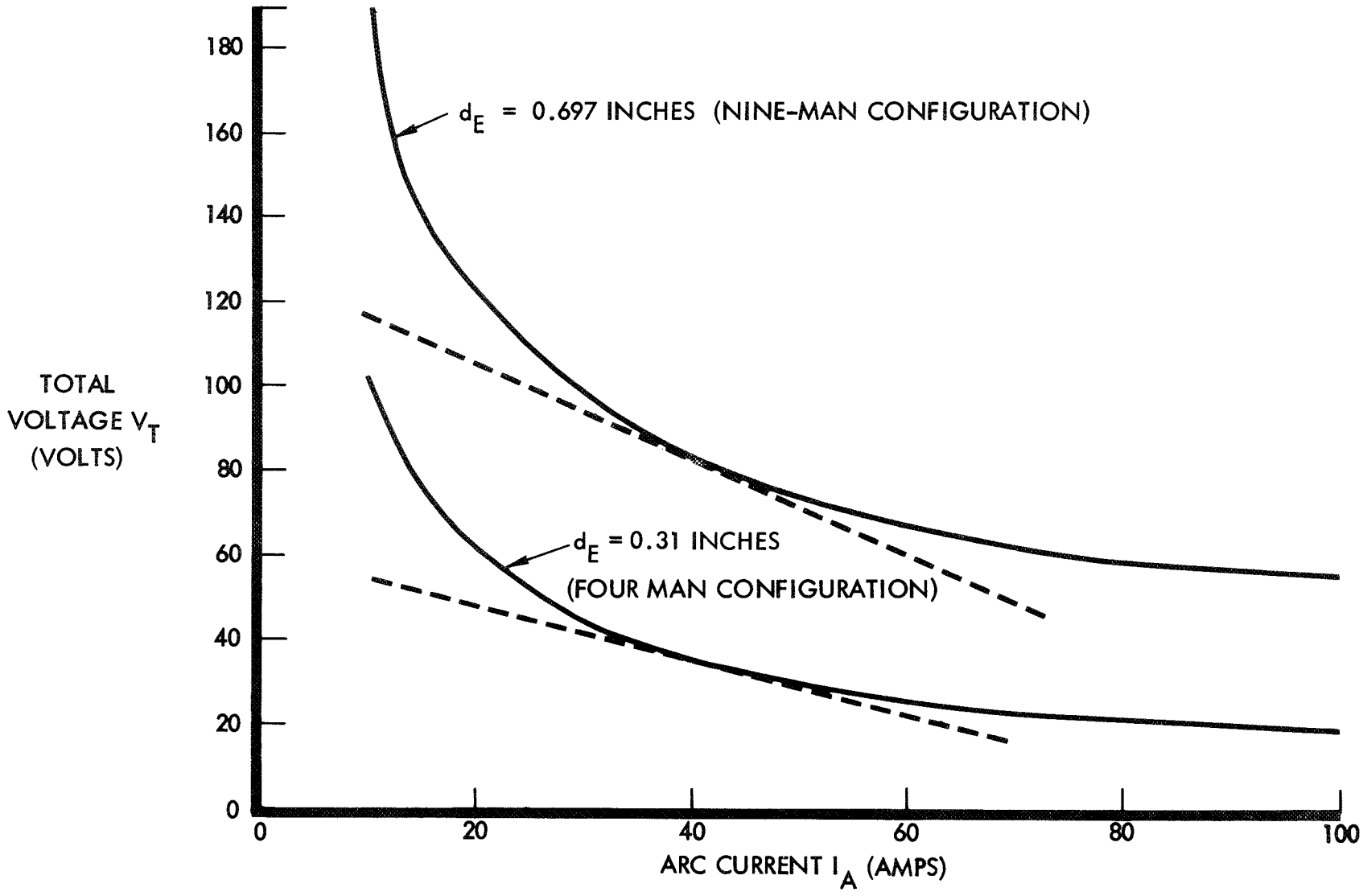

Figure 4.5: VOLTAGE - CURRENT CHARACTERISTIC OF HYDROGEN ARC HEATER

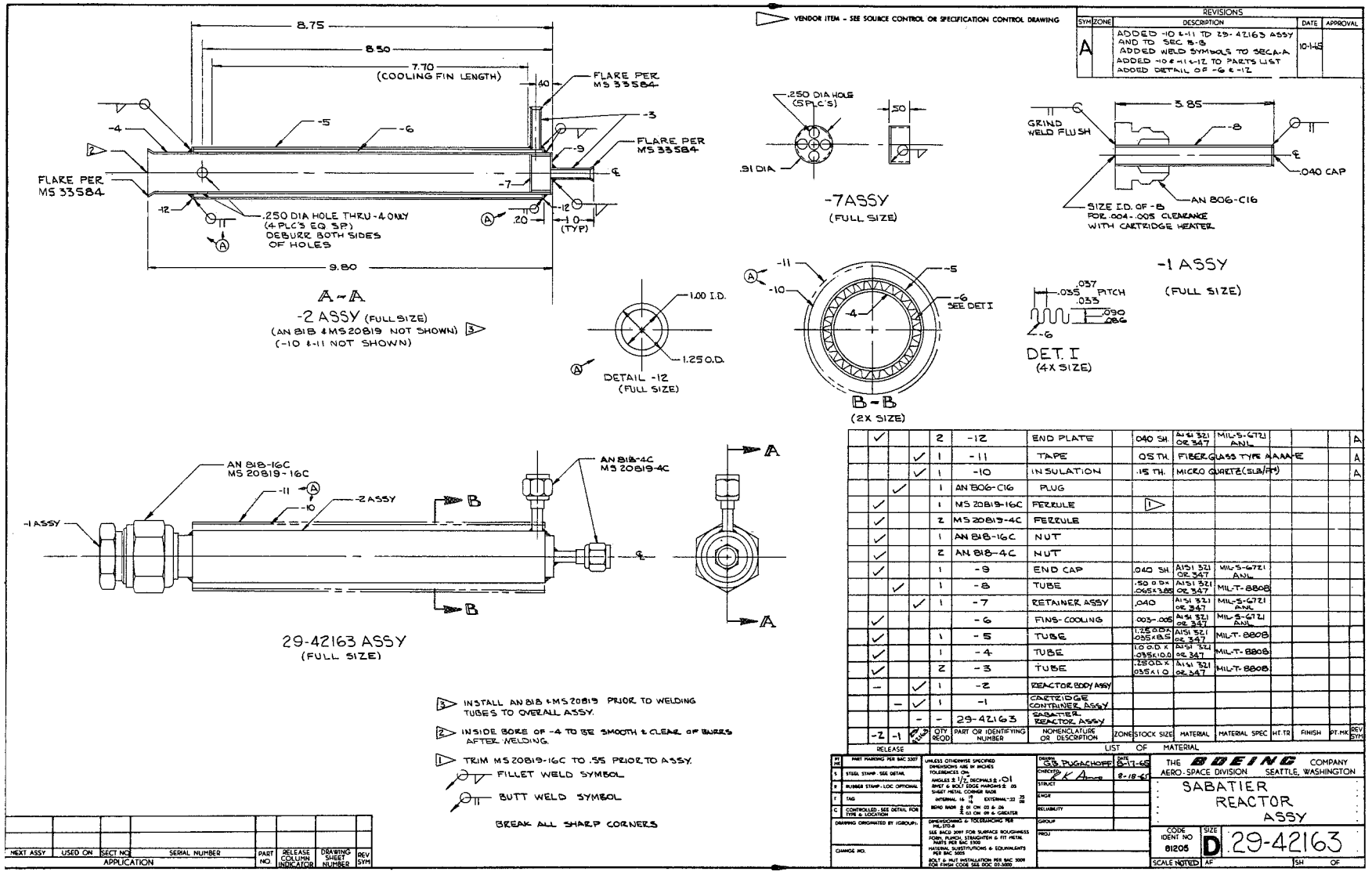

Figure 5.1: SABATIER REACTOR ASSEMBLY

angle to the main reactor body. The gases then pass through the heat exchanger fins where heat is transmitted from the catalyst heated by the exothermic Sabatier reaction. The gases enter the catalyst area through access holes and are heated by the electric heater which is projected into the catalyst bed. The gases pass through the catalyst bed and out the flared tube fitting located axially to the reactor body. A high density heater, Watlow-Firerod, was used in the reactor heater container. Local heater surface temperatures during the reactor start-up were calculated to be between 1000 and 1200°F.

Three Sabatier reactors were designed and constructed for use in previous reaction studies conducted by Boeing. These reactors were analyzed for possible use for the 4-9 man system under study. They were found to be adequate, especially with the high (30%) excess of hydrogen expected to be used in the reactor feed. Space velocities in the vicinity of 4000 hr^{-1} at the highest flows were predicted. Previous tests with similar Sabatier reactors indicated CO_2 conversion efficiencies of 99.5% or higher at 30% hydrogen excess. The reactors were plumbed in parallel (see Figure 5.2) and instrumented for thermal analysis. The reactors are essentially identical to drawing SK29-42163, Figure 5.1.

6.0 TEST SETUP

A test cell was constructed to contain the plasma reactor and Sabatier reactor, confining the possible spread of fire due to mishap. Figure 6.1 shows the cell interior with the plasma reactor plumbed for cooling water temperature control; the Sabatier reactors (plumbed in parallel); a wet test gas flow meter used to monitor both Sabatier and plasma reactor gas flows; a Fluke 845 AB Voltmeter for ΔT measurement of the plasma reactor water coolant segments; a high volt igniter used to implant a starting spark (45 to 50 K volts); a water condenser - separator to remove water formed by the Sabatier reaction; and temperature recorders to monitor Sabatier reactor gas feed and exhaust temperatures, and reactor wall temperatures.

A view from outside the test cell (Figure 6.2) shows supporting equipment including: a Sanborn 320 D.C. amplifier-recorder used to monitor and measure the plasma reactor volt-amp performance; an ignition switch used to start the plasma reactor from outside the test cell; two Christie Electric MHX-2500 4C-Solid State power supplies connected in series for supply and control of power

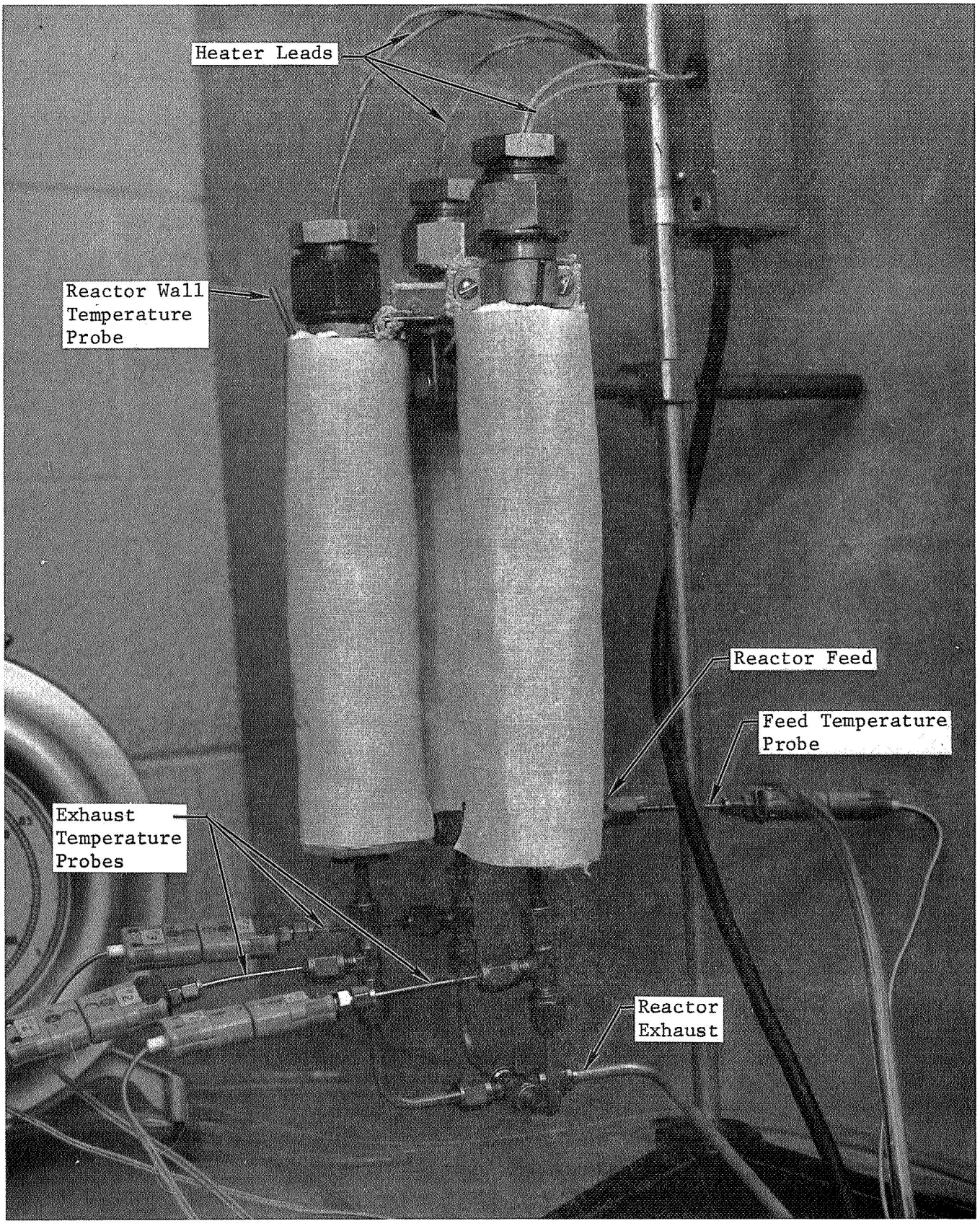

Figure 5.2: SABATIER REACTOR

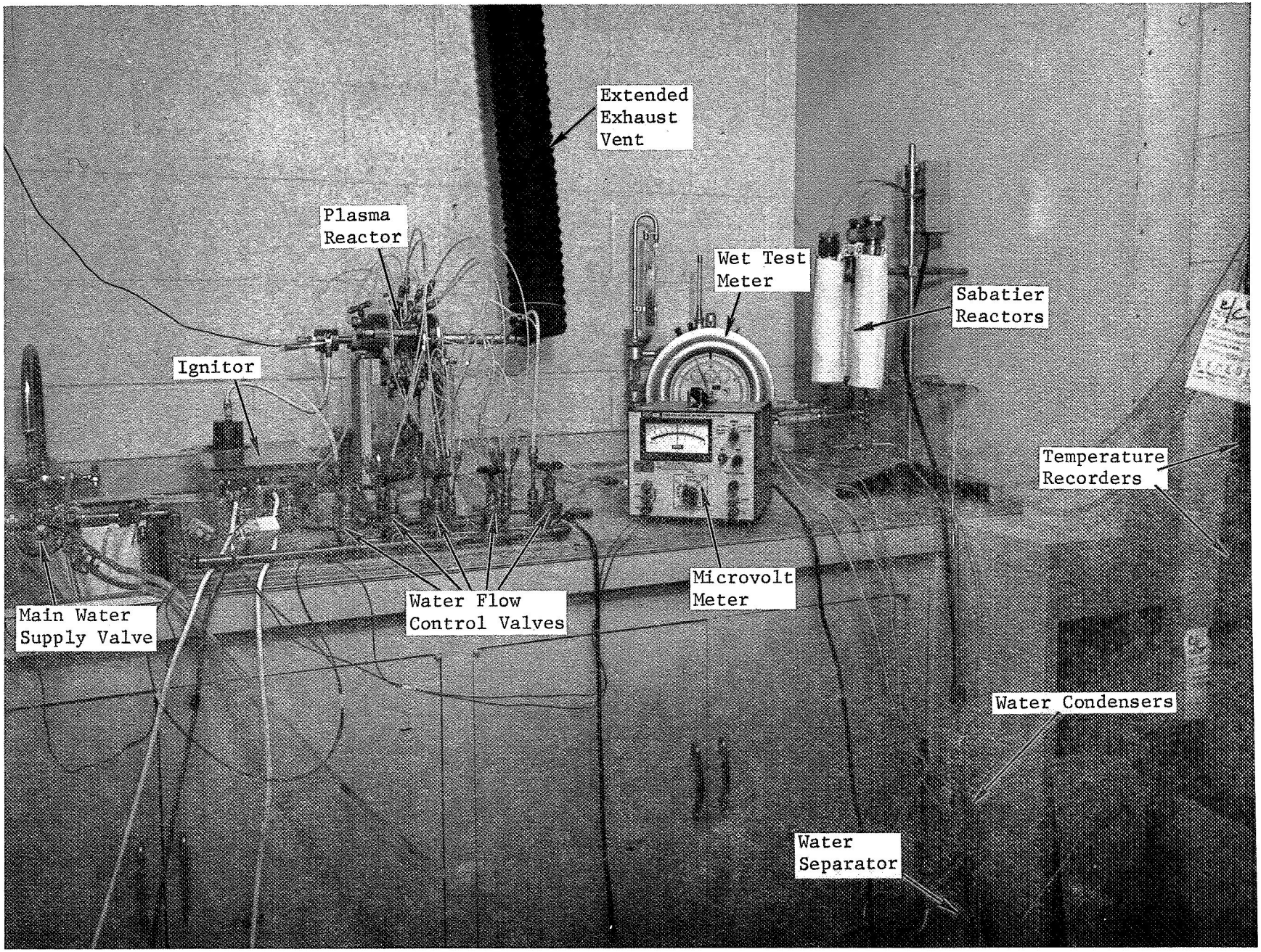

Figure 6.1: TEST SETUP

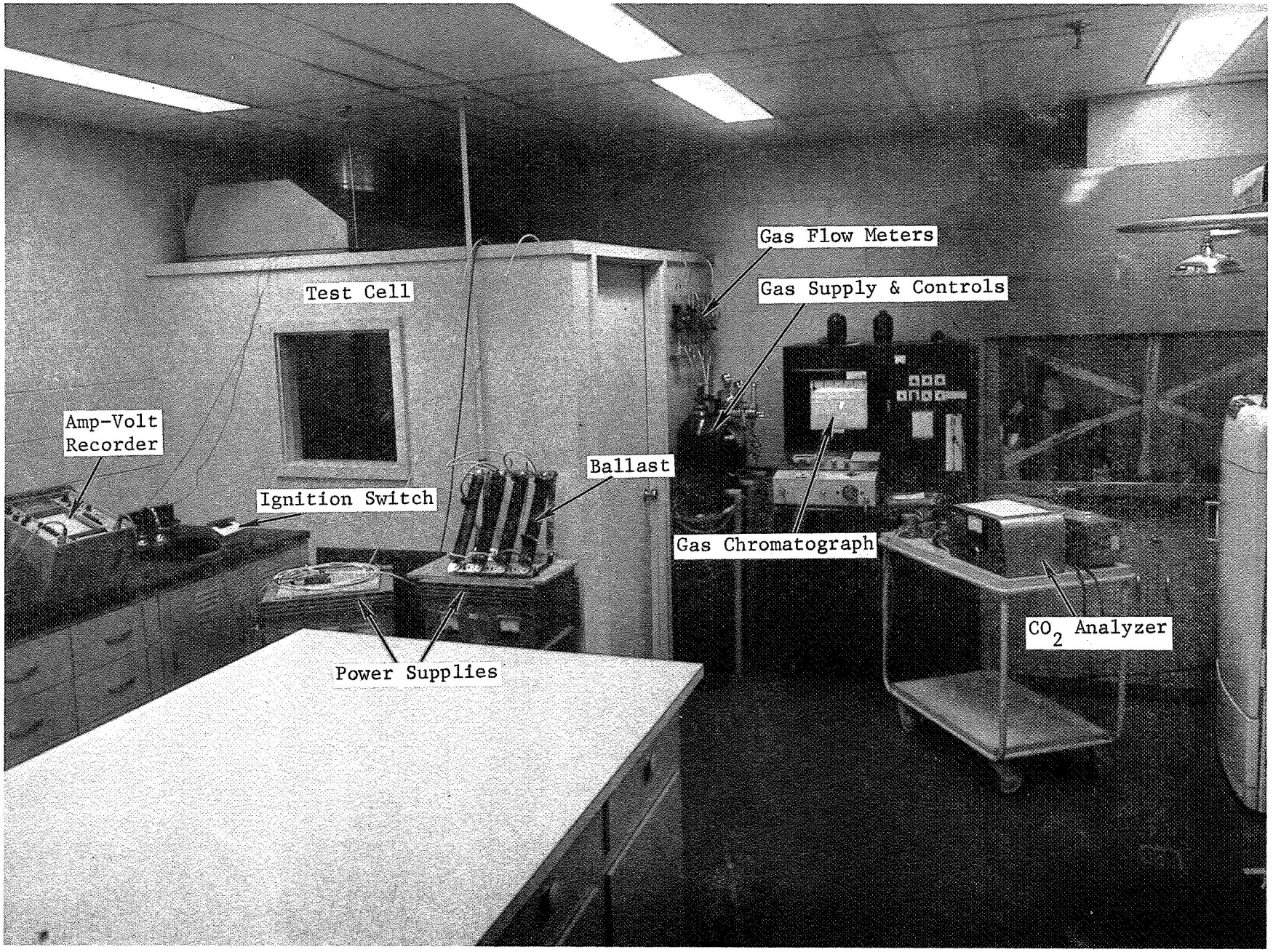

Figure 6.2: TEST SETUP

to the plasma reactors; a resistance ballast for providing better power curve characteristics control; hydrogen, argon, carbon dioxide gas bottles of high purity with appropriate pressure controls and valves to regulate gas flows to the Sabatier and plasma reactors; calibrated flow meters to monitor feed gas flows; a GC-1 Beckman gas analyzer used to measure the test gas constituents; and a Beckman 4B infrared analyzer (Model 15A) for continuous monitoring of carbon dioxide when deemed necessary. With the test setup described, it was possible for one man to set test conditions and operate the reactors to obtain test data.

7.0 SABATIER REACTOR PERFORMANCE

The Sabatier reactors were operated at the four-man system flow rates and "tuned" for optimum operation by adjusting reactor insulation. Figure 7.1 shows the reactor performance for a carbon dioxide feed of 9.00 pounds per day and a hydrogen feed of 1.635 to 2.12 pounds per day. This represents a feed ratio from stoichiometric to 30% hydrogen excess. The system was run at 30% hydrogen excess using approximately 200 grams of 20% ruthenium on alumina catalyst (Lot C-4955) as supplied by Engelhard Industries. A carbon dioxide conversion efficiency of 99.89 percent was obtained.

Reactor startup was accomplished within nine minutes using a 150 watt heater and gas flow at stoichiometric ratios. Thermal profiles along the outer surface of the reactors indicate a high temperature of 790°F at stoichiometric gas flow and temperatures of 805, 820, and 827°F , respectively at 10, 20 and 30% excess hydrogen flows. Insulation consisted of a single wrap of one-half inch unbonded Microquartz ® over the full nine inch length of the reactors.

The Sabatier reactors were operated at the nine-man system flow rates to determine the change in insulation required to optimize the reaction. Figure 7.2 shows reactor performance over a hydrogen feed rate of stoichiometric to 30% excess using a CO_2 feed rate of 20.25 pounds per day. Maintaining the same insulation configuration as used for the four man system, the reactors ran consistently hotter than desired (1005°F at the highest point) and CO_2 conversion efficiency reached a maximum of 93.3%.

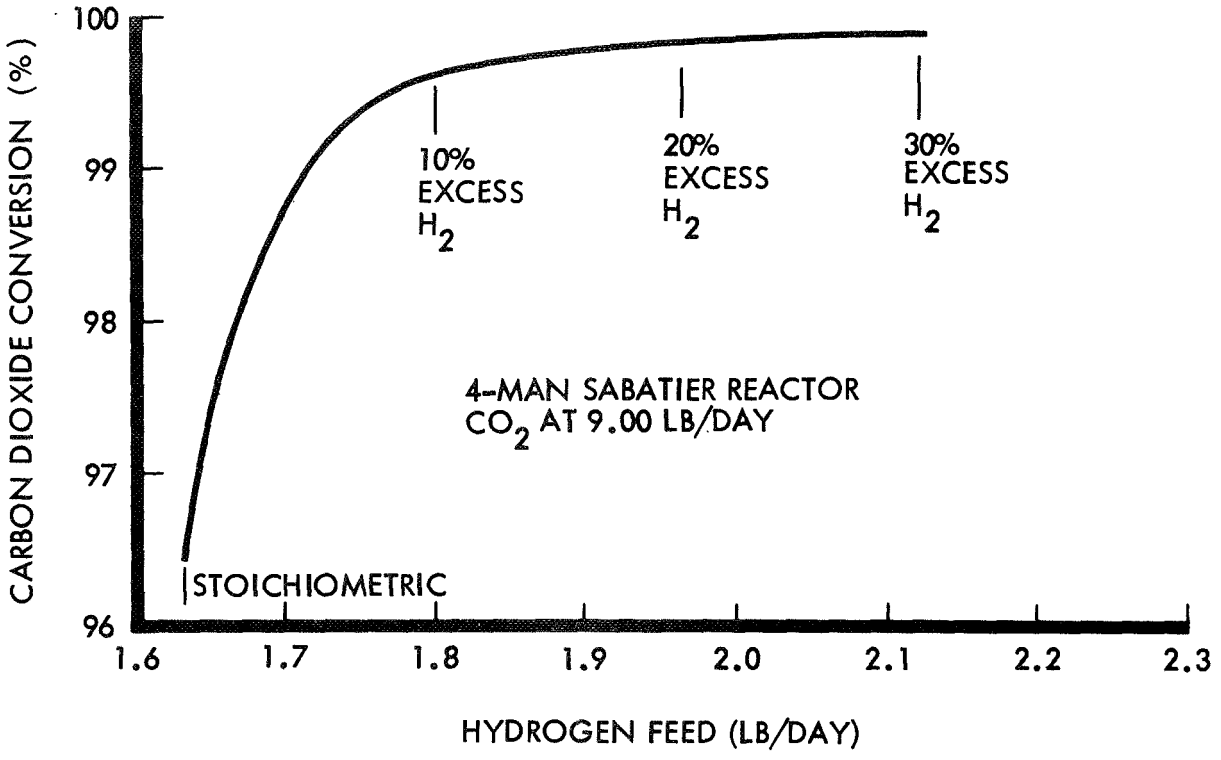

Figure 7.1: SABATIER REACTOR PERFORMANCE - FOUR-MAN SYSTEM

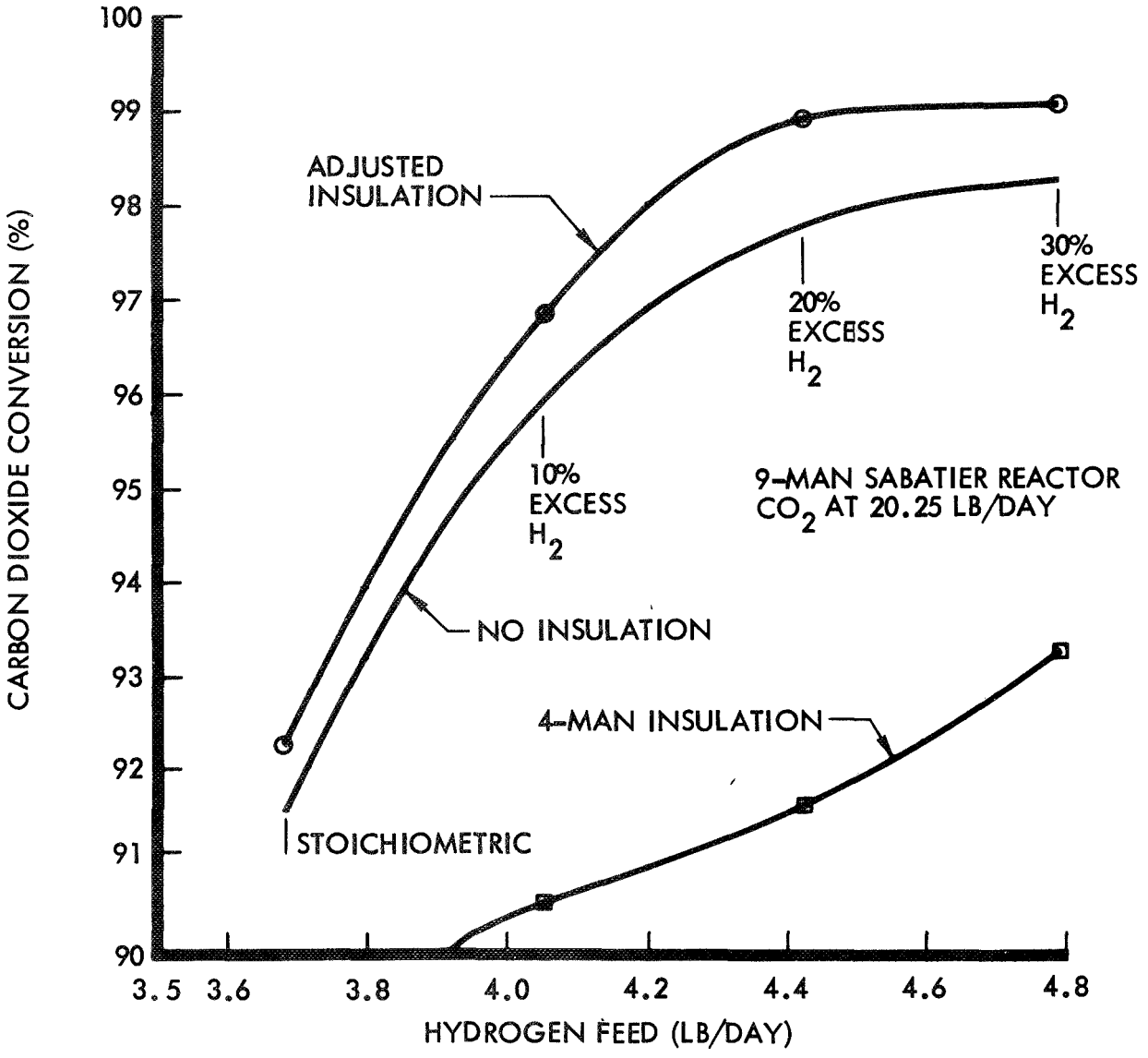

Figure 7.2: SABATIER REACTOR PERFORMANCE - NINE-MAN SYSTEM

Running the reactors without insulation produced better results with CO_2 conversion efficiency reaching a maximum of 98.24%. However, the bulk temperature of the reactor was lower than desired. Further improvement of performance was achieved by partial insulation of the reactor as shown below.

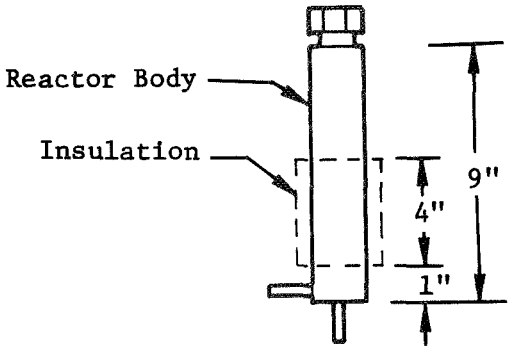

SCHEMATIC OF ADJUSTED INSULATION

With a single wrap of one-half inch unbonded Microquartz ®, , the performance improved to a maximum of 99.02% CO_2 conversion efficiency.

A comparison of the Sabatier reactor performance normalized for excess % hydrogen is shown in Figure 7.3. The nine man flow rates are reaching the limits of the reactors efficiency, and an additional reactor would raise the total efficiency. It should be noted that the expected operation at 30% H_2 excess was over 99% CO_2 conversion efficiency at both the four and nine man flow rates.

8.0 PLASMA REACTOR PERFORMANCE

Performance development of the reactor required the establishment of the geometric and electrical operating parameters to obtain a stable hydrogen plasma, and then an optimization of the anode design to maximize the energy available downstream of the anode for the methane reaction.

8.1 INITIAL TESTS

Initial tests were conducted with a cathode-anode spacing of 0.31 inches using the anode shown in Figure 4.1. (See Figure 8.9 for comparison of anodes

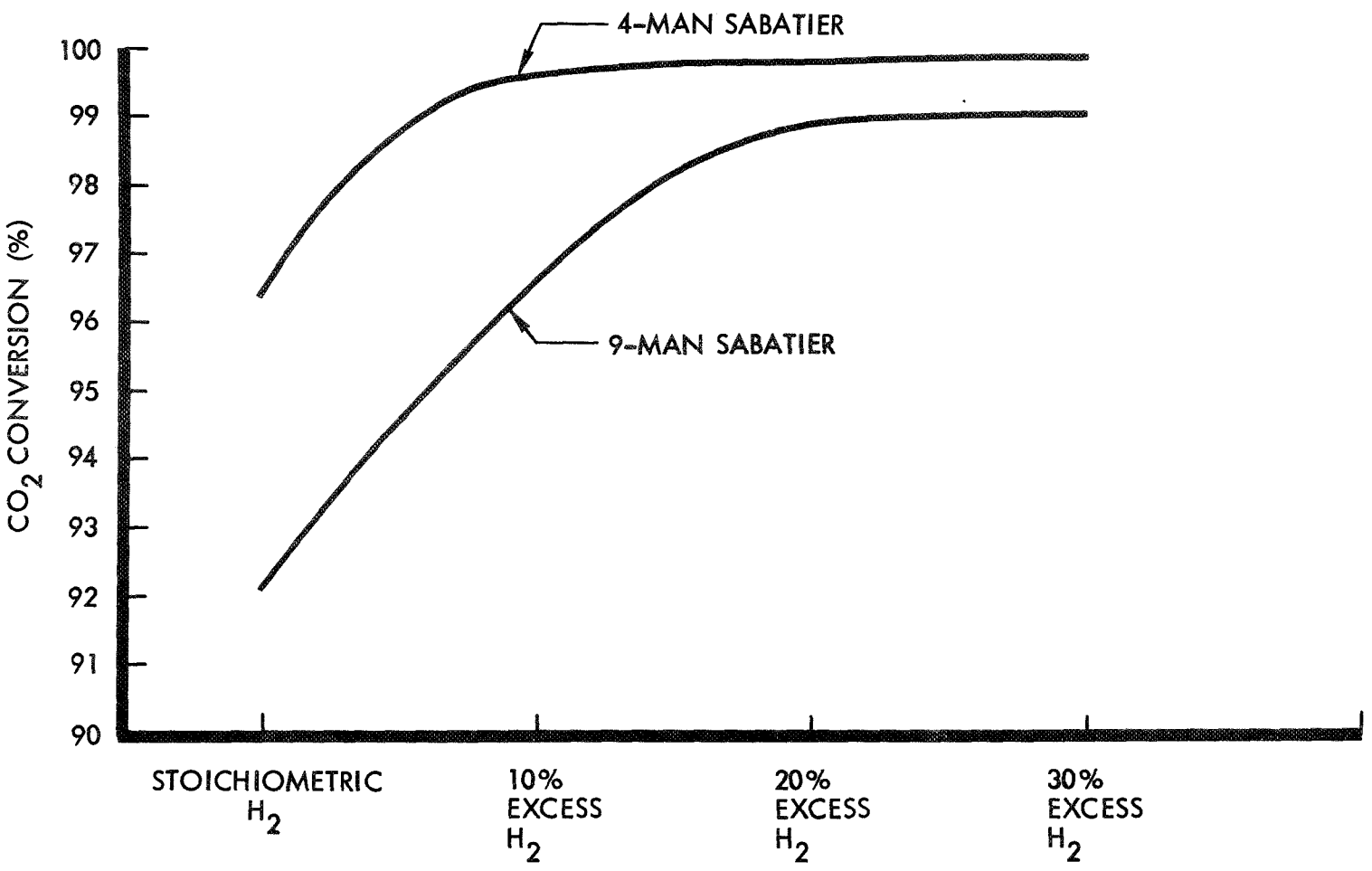

Figure 7.3: SABATIER REACTOR PERFORMANCE

used in the test program.)

The plasma reactor was operated successively with argon, argon-hydrogen, and hydrogen feeds into the cathode. Also, the downstream methane feed ring was cooled by adding either argon or hydrogen gas. A stable plasma was not obtained when the last trace of argon gas was removed from the system.

Figure 8.1 shows typical results of initial tests running the plasma reactor with argon-hydrogen feed. The cathode-anode spacing was set at 0.31 inches and hydrogen flow was set at 0.705 liters per minute.* Argon flow was 0.3 liters per minute; the lowest flow rate that would still provide a stable plasma. The plasma volt-amp characteristics show an angle of 52^{o} between the plasma and the 40 amp control line. A ballast of 0.5 ohms placed in series with the plasma was required to obtain stable operation. Unfortunately, this placed the total power curve (Plasma + Ballast) in the upper limits of the power supply.

Additional tests were run with a 1.0 ohm ballast and zero argon feed into the cathode (Figure 8.2). The desired hydrogen feed rate (0.705 liters per minute) could not be reached using the available power supply. Data obtained at lower flow rates of hydrogen projected to the desired flow rate is shown in dashed lines. This projection indicated 78 volts at 40 amps versus the predicted 48 volts at 40 amps. Adding ballast resistance to provide a stable plasma pushed the performance volt-amp characteristics outside the controlling regime of the power supply. At this point, it was decided to stop the program until a new power supply with greater capacity could be obtained, so that testing could continue in an operable power supply regime.

A new power supply identical to the original was obtained and connected in series increasing the voltage capacity to 130 volts over the same amperage range (0-100). This combination of power supplies was used during the remainder of the test program.

---

* Flows corrected to standard pressure and temperature.

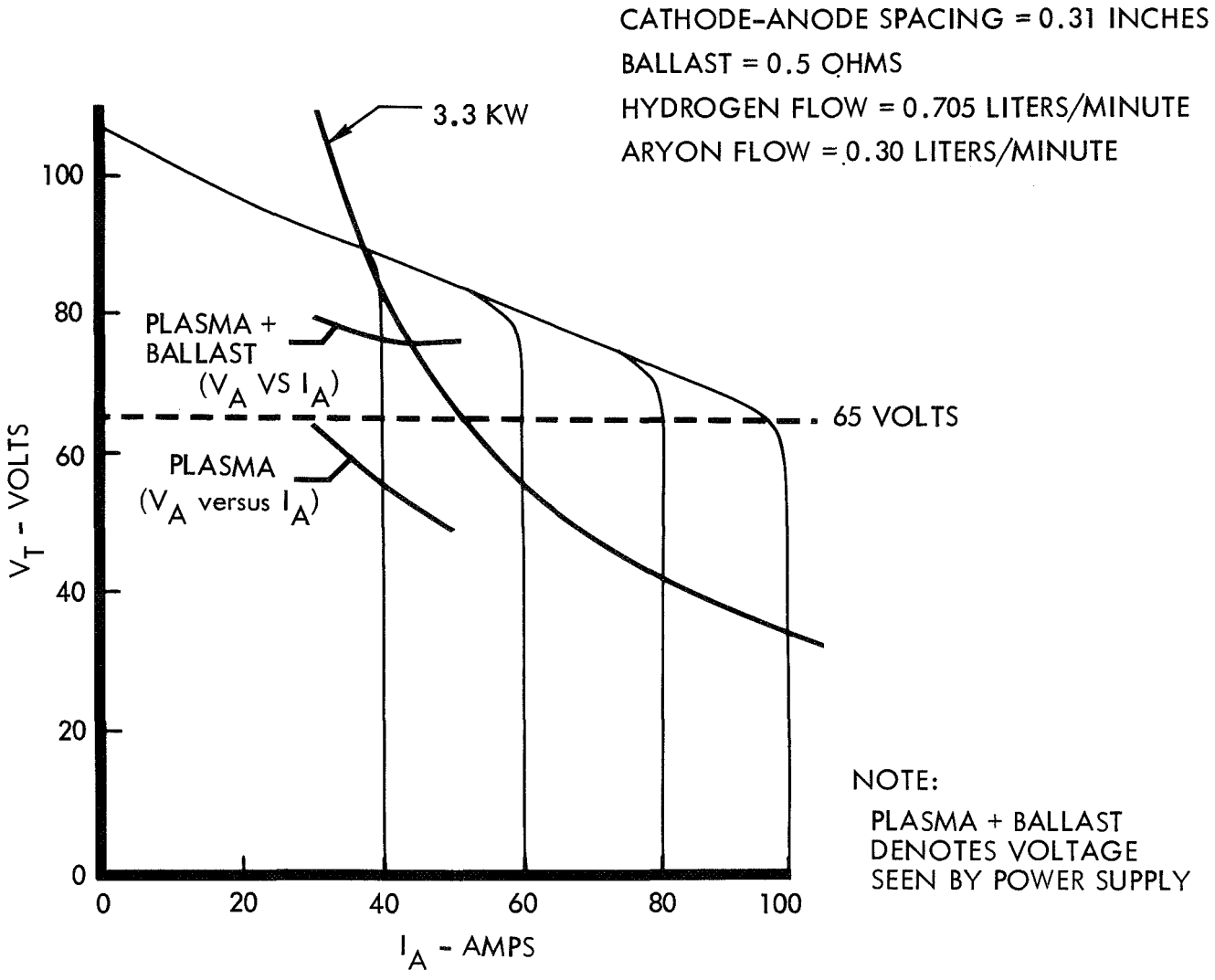

Figure 8.1: PLASMA CHARACTERISTICS WITH H_2 - A FEED

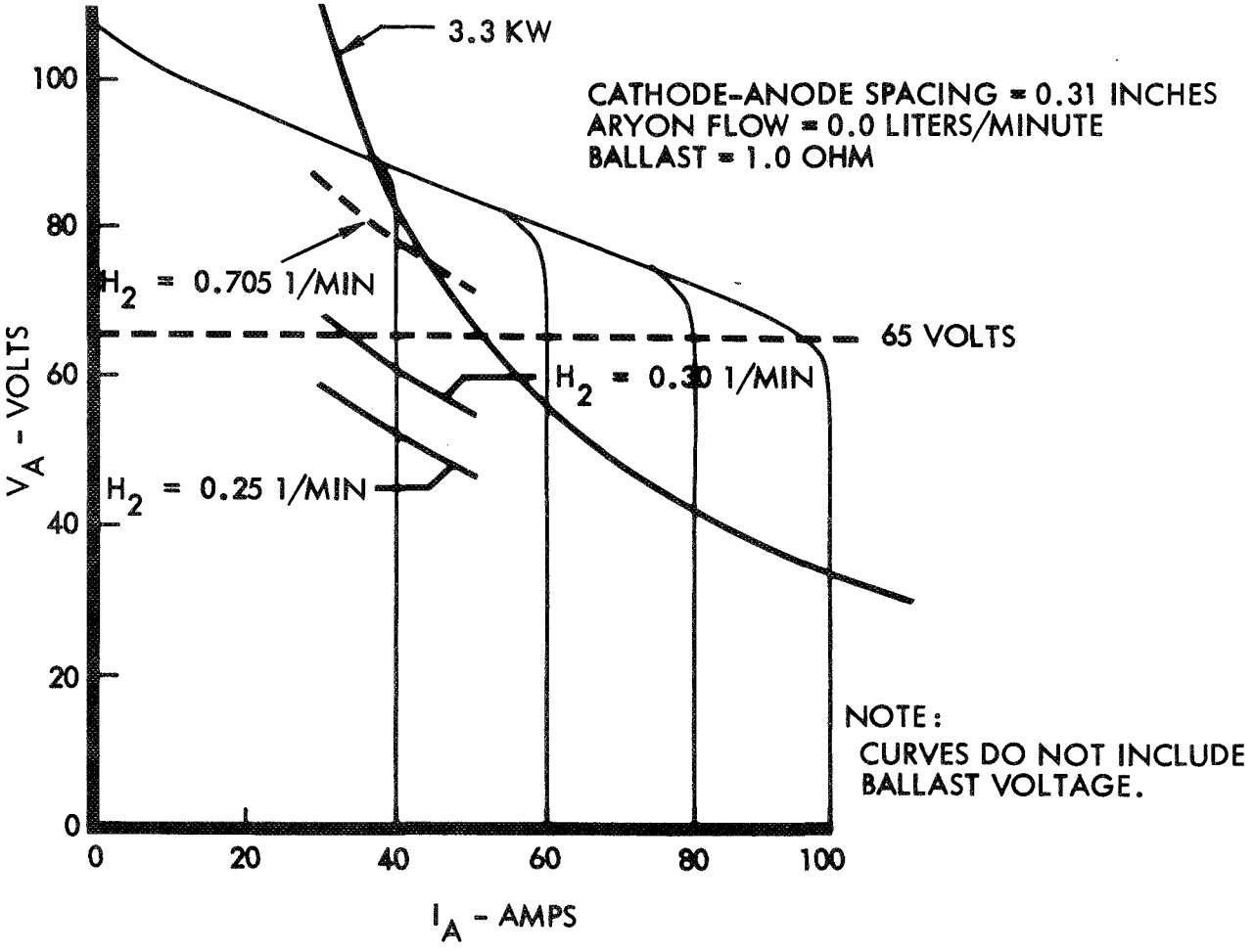

Figure 8.2: PLASMA CHARACTERISTICS WITH H_2 FEED

8.2 ORIGINAL ANODE TESTS

The anode as previously described was operated at higher ampere levels with pure hydrogen. The orifice size (0.25 inches) had a great effect on arc stability. Pure hydrogen arcs at the power level under investigation had an overriding tendency to attach at a single point. Even with gas feed into the cathode region at a tangent (vortex), the arc did not tend to move smoothly around the orifice. This was accentuated when the orifice size was relatively large. The reactor was operated as shown in Table 8.1.

Table 8.1: ELECTRO-OPTICAL ANODE OPERATING PARAMETERS

Cathode Anode Spacing Inches	V_A (Volts)	I_A (Amps)
0.115	56	62 Split Attachment
	68	61 Single Attachment
0.20	60	62 Split
	70	61 Single
0.30	70	62 Erractic Attachment

Hydrogen flow rate was 0.705 liters/minute, and a ballast of 1.0 ohms was used to stabilize the plasma. The arc would tend to attach at a single point for a while, and then split attachment (usually to two locations). The split attachment would move from one point to another and back at very high (8000 cps) frequencies.

At a cathode-anode spacing of 0.30 inches the distance required for the arc to move seemed too great, and an erratic point-to-point movement was observed. Small amounts (0.075 liters/min.) of argon in the hydrogen feed had a strong stabilizing effect. The use of a magnetic field was attempted to influence plasma movement or stability. An 800 wrap coil was located axially to the anode and operated at 1 amp-24 volts d.c. The magnetic field generated did tend to force rotation of the arc, but did not produce any stabilizing effect. A slight increase in plasma arc voltage (1-3 volts) was observed.

An attempt was made to operate the anode on pure hydrogen with Sabatier exhaust feed at a four-man rate of 2.00 liters/minute at 70°F, 1 atm. Gas composition was: CH_4, 79.0%; H_2, 20.7%; CO_2, 0.15%; O_2 and N_2 trace. Cathode-anode spacing of 0.20 inches and plasma hydrogen feed of 0.705 liters/minute produced a plasma of 70 volts - 61 amps with a single arc attachment. Sabatier exhaust was fed downstream of the anode. The resulting back mixing of the methane into the cathode region resulted in a near catastrophic erosion of both the cathode and anode (see Figure 8.3). The test had to be terminated. Amp-volt recordings showed a highly erratic operation. Subsequent conversation with Dr. Thomas Reed, Lincoln Labs, M.I.T., revealed that hot tungsten reacts with organic gases. The mechanism is not known but it is estimated that some carbides are formed in the process.

8.3 REVISED ANODE TESTS

A second anode was obtained from Electro-Optical Systems designed to reduce the back mixing problem. The anode was similar with the exception of orifice size, reduced to 0.1 inches in diameter (Figure 8.4). A stable pure hydrogen plasma was obtained at 0.20 inches cathode-anode spacing. Nominal plasma operating values were 50 to 54 volts at 63 amps with 0.705 liters/minute hydrogen flow and 1.0 ohm ballast. Operation of the plasma with Sabatier feed into the plasma downstream of the anode did not produce measurable acetylene formation.

Tests were then conducted to determine reactor plasma generation efficiency, balancing energy input (watts) versus energy output in the cooling water. Results of two test cases are shown in Table 8.2.

Table 8.2: PLASMA REACTOR EFFICIENCY

Cathode Anode Spacing (inches)	V_A (Volts)	I_A (Amps)	Energy Into Reactor (Kw)	% Energy into Cooling Water			
				Cathode	First Constrictor Section	Anode	Second Constrictor Section
0.20	44	63.5	2.795	8.98	13.93	72.75	4.34
0.30	56	54	3.020	10.27	20.11	65.70	3.92

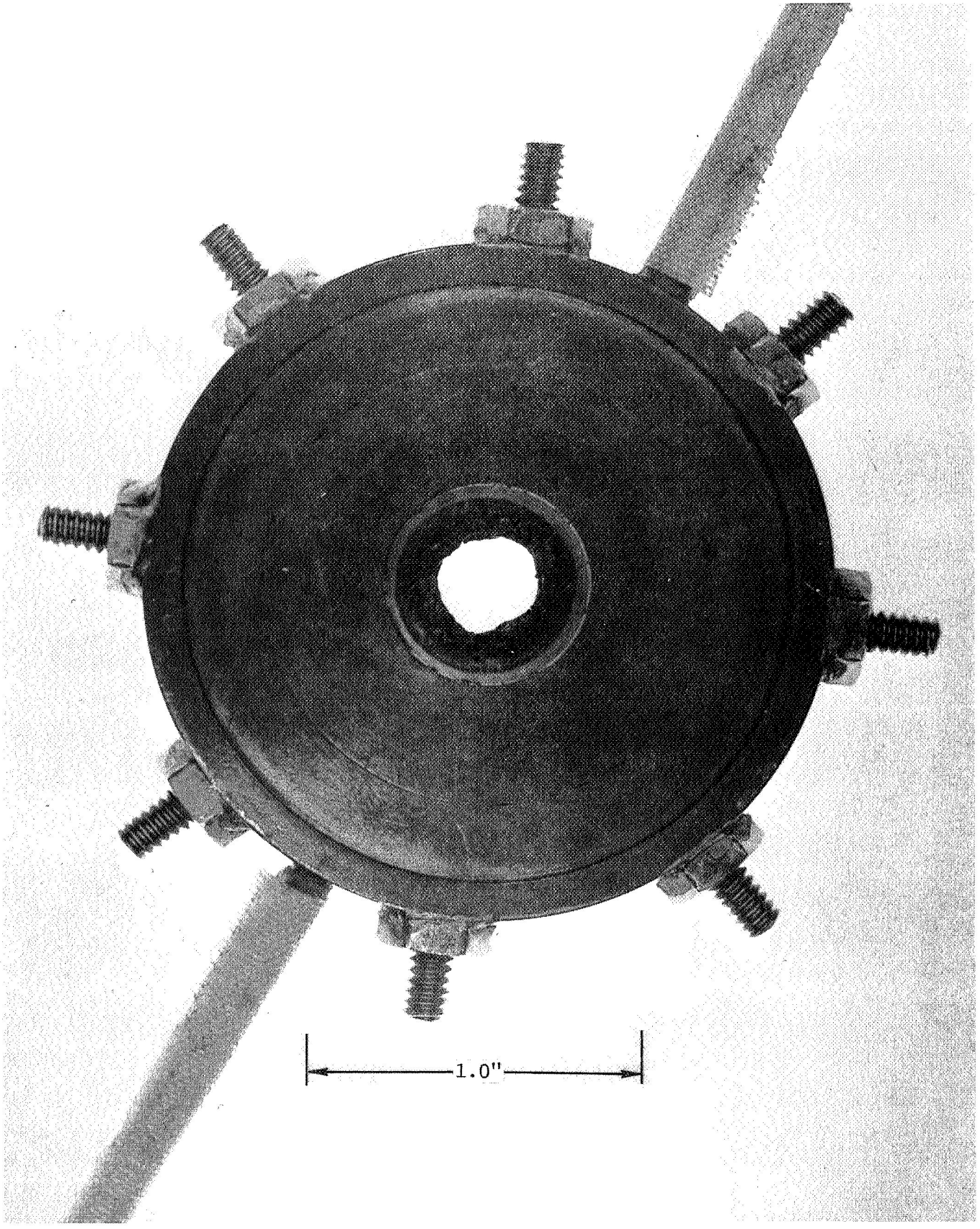

Figure 8.3: ORIGINAL ELECTRO-OPTICAL ANODE

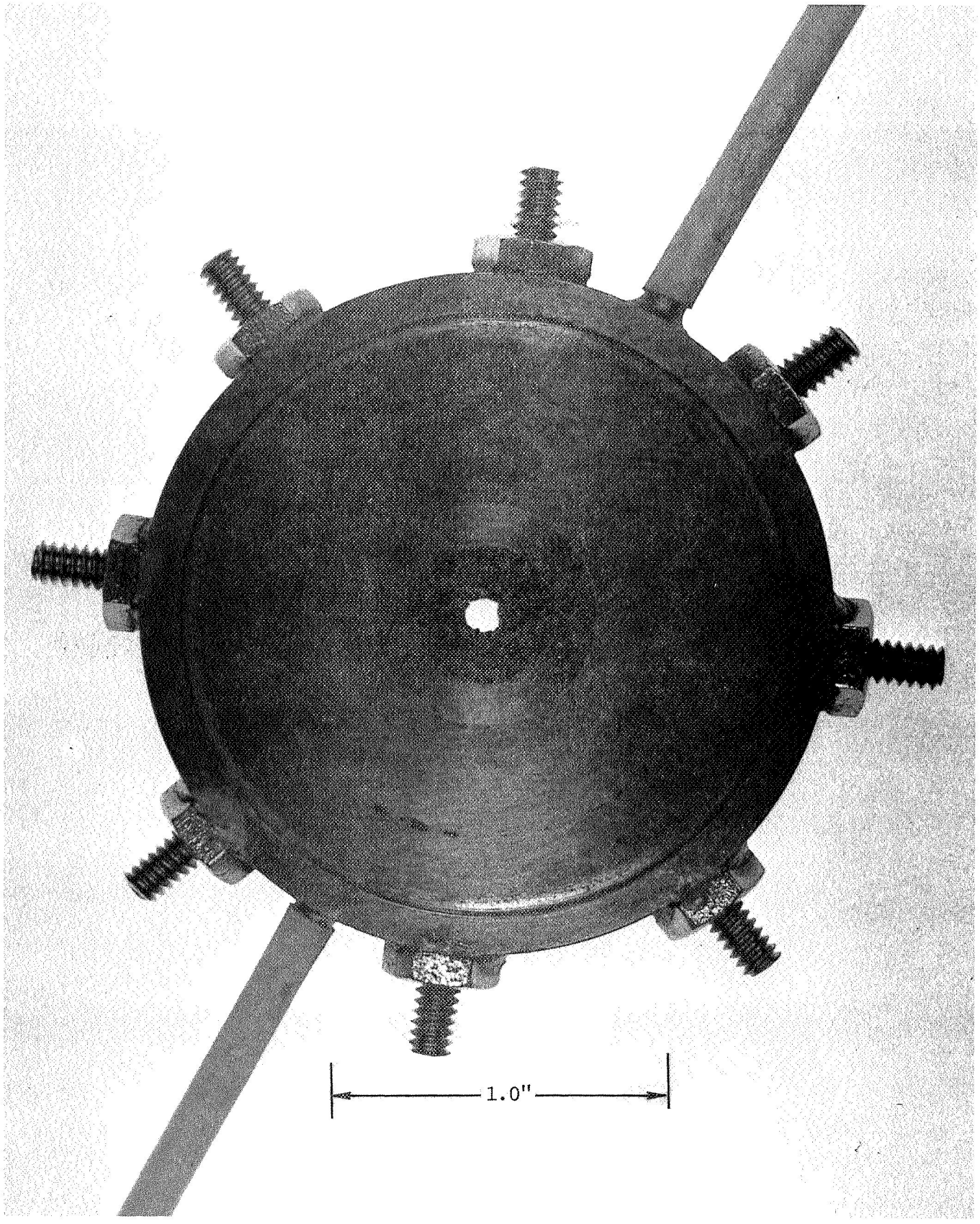

Figure 8.4: ELECTRO-OPTICAL ANODE (Revised)

The results are graphic in showing a major design problem in respect to energy loss to the anode. The anode was running cool, and thus conductive losses were much greater than desired. Losses to the anode should not be greater than 40-50% and many plasma devices similar to this, but at a higher total energy level, operate with as low as 30% losses to the anode.

After analyzing the energy data, it was not surprising that downstream reactions were not evidenced, as only 4% of the energy input was available for the methane reduction process, providing a downstream gas temperature too low to effect methane reaction.

8.4 HIGH TEMPERATURE ANODE

8.4.1 Design

It was decided that a new anode design was required that would limit the energy that could be removed by cooling, by raising the orifice temperature to 3500-4000°F. This would also promote a more diffuse arc attachment as the orifice reached incandescent temperatures.

A thermal analysis of the anode configuration was made to determine design parameters for a new anode. Assuming that conductive heat transfer is controlling, and loss of energy by radiation from the exposed anode surface is small, the analytical model shown below was developed.

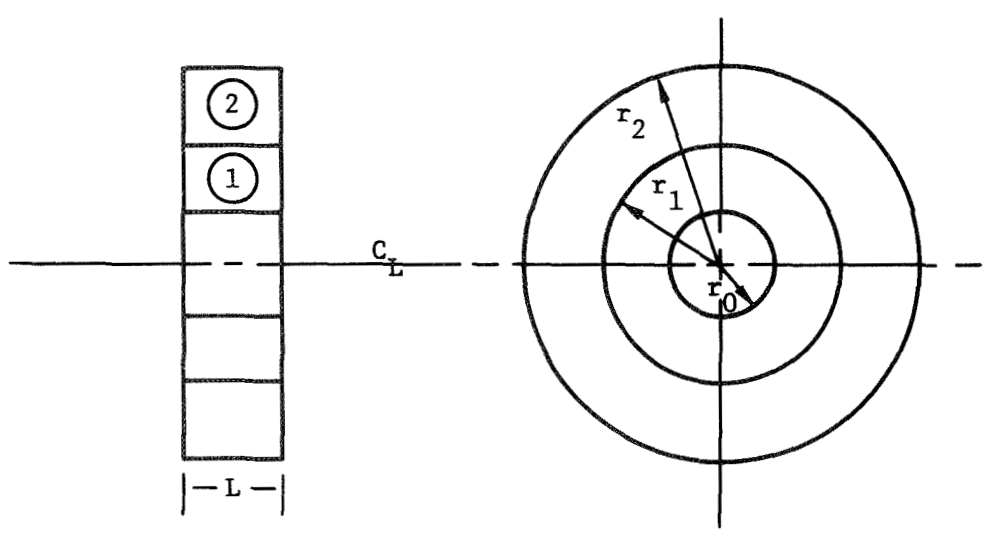

Let:

T_0 = Temperature at $r = r_0$

T_1 = Temperature at $r = r_1$

T_2 = Temperature at $r = r_2$

K_1 = Thermal conductivity of material ①

K_2 = Thermal conductivity of material ②

Q = Heating rate at $r = r_o$

For one dimensional radiation conduction:

$$T_0 - T_1 = \left(\frac{Q}{2\pi L K_1}\right) \log_e \left(\frac{r_1}{r_0}\right)$$

Similar relations would hold for any number concentric materials.

T in 10^3 ^oR

Q in Kilowatts

L in inches

K in BTU/FT-HR-^oR

$$T_0 - T_1 = \left(\frac{6.51Q}{LK_1}\right) \log_e \left(\frac{r_1}{r_0}\right)$$

A series of plots of $\frac{r_1}{r_0}$ vs. T_1 was made for $T_0 = 3500^oF$. $L = 0.35$ to .05 inches, $K_1 = 60$ BTU/FT-HR-^oF (tungsten) and $Q = 1$ KW (approx. 40% of total expected arc energy) and are shown in Figure 8.5.

The selected design point for the tungsten insert was $L = 0.13$ inches and $T_1 = 2200^oF$. Thus, a 0.5 inch diameter tungsten insert with 0.10 inch diameter hole will give the desired T_1 of 2660^oR, which is the limiting junction temperature for a 304 stainless steel holder. Also, assuming:

$T_2 = 520^oR$, $K_2 = 12$ BTU/FT-HR-^oR

$L = 0.13$ inches

$Q = 1$ KW

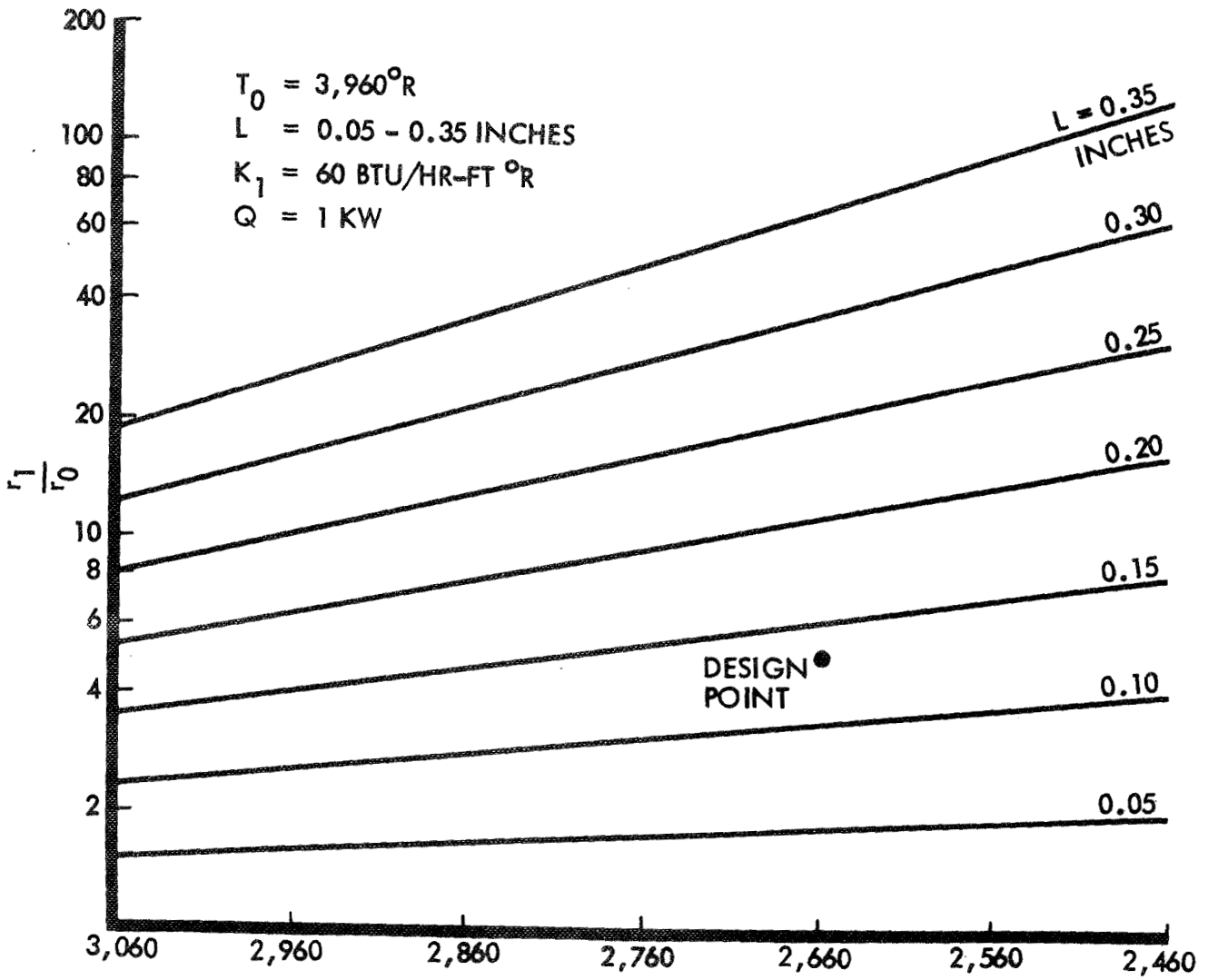

Figure 8.5: HIGH TEMPERATURE ANODE DESIGN

$$\frac{r_2}{r_1} = \exp\left[\frac{LK_2}{6.51Q}(T_1 - T_2)\right]$$

$$\frac{r_2}{r_1} = \exp\left[\frac{(0.13)(12)}{(6.51)(1)}(2.14)\right] = e^{0.513} = 1.67$$

$$r_2 = 1.67\ (0.25) = 0.417 \text{ inches}$$

This provides the remaining design parameters, limiting the water cooling radius design as shown in Figure 8.6

8.4.2 First Configuration Tests

An anode was constructed by Electro-Optical Systems as shown in Figure 8.6 with the exception that the tungsten thickness was reduced to 0.07 inches and the orifice diameter was 0.07 inches. Tests were performed to determine reactor efficiency, balancing energy input to the reactor versus energy output to the cooling water. Results of the test are shown in Table 8.3. The reactor was operated with pure argon, and then with argon-hydrogen mixtures until the full hydrogen flow (0.705 liters/minute) was obtained. A subsequent reduction in argon flow, keeping hydrogen flow constant, resulted in anode overheating, melting the orifice area to approximately 0.2 inches in diameter (Figure 8.7). Comparison of data from Table 8.3 and that presented in Table 8.2 shows a dramatic increase of energy into the gas downstream of the anode, and a resulting decrease in energy lost to the anode. The highest energy level (6286 BTU/HR) indicated the distribution of energy to be: Cathode 10.1%, First Constrictor section 15.8%, Anode 53.1%, and Second constrictor section 21%.

It became obvious that the geometric sizing of the anode was extremely critical, and must be designed to allow the orifice to reach incandescent temperatures but not to melting temperatures.

8.4.3 Second Configuration Tests

A new anode with web thickness 0.13 inches and orifice diameter 0.08 inches was made. The tungsten insert was electron beam welded to the stainless steel

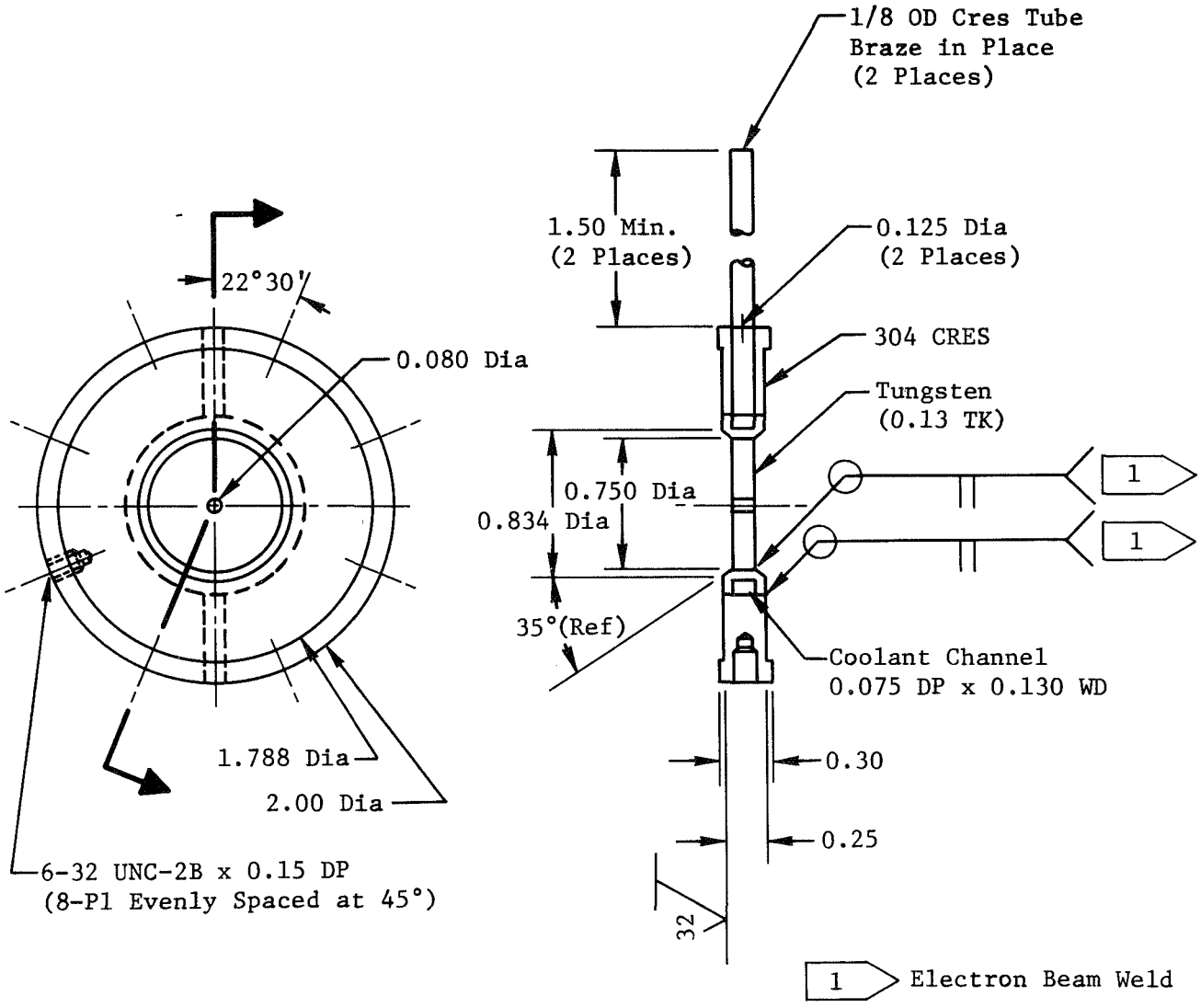

Figure 8.6: HIGH TEMPERATURE ANODE

Table 8.3: PLASMA THERMAL BALANCE DATA

Gas Flow (L/min)		Energy Output (btu/hr)				
H_2	A	Cathode	First Constrictor	Anode	Second Constrictor	Total
0.0	0.63	523	363	1466	352	2704
0.24	0.63	635	761	2600	540	4536
0.37	0.63	638	890	2865	564	4957
0.53	0.63	623	890	3135	728	5376
0.705	0.63	638 (10.1%)	990 (15.8%)	3335 (53.1%)	1323 (21.0%)	6286 (100%)

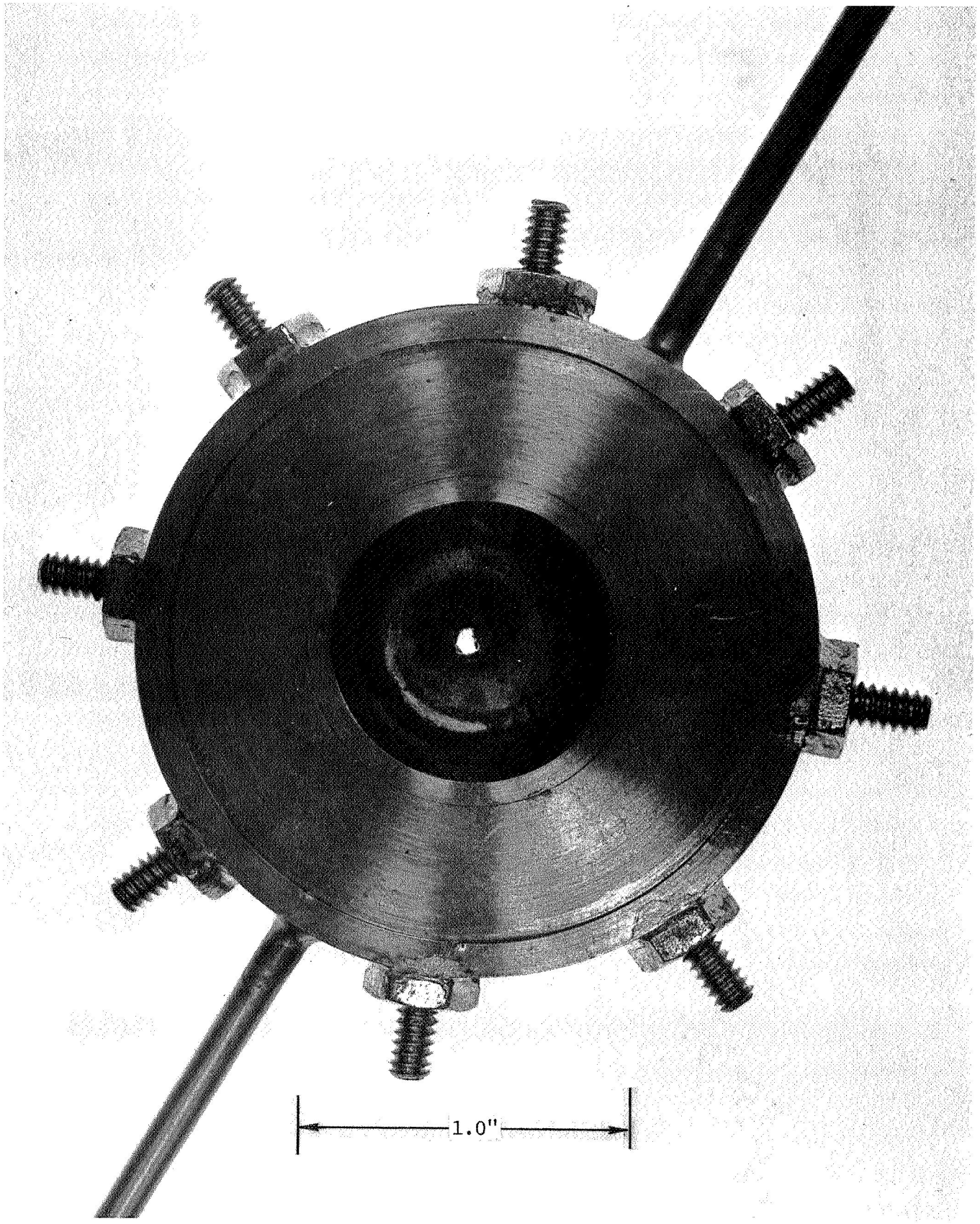

Figure 8.7: HIGH TEMPERATURE ANODE
(0.07 Inches Web Thickness)

holder (as shown in Figure 8.6). Data similar to that described in Table 1 was being obtained when one of the two power supplies (in series) shut down, extinguishing the arc. Upon re-start, a water leak on the downstream side of the anode was observed, and the test was stopped to examine the anode. Upon examination, it was apparent that the mechanical forces of heating and sudden quenching resulted in separating the silver solder seal (around the water jacket) from the stainless steel resulting in a water leak.

To eliminate this problem, a new anode of the same dimensions was built with all seams and junctions electron beam welded. In this manner, the expansion-contraction forces were distributed throughout the anode. This anode was tested with hydrogen-argon mixtures and finally with pure hydrogen without mechanical failure or anode burn-out. The cathode-anode configuration for the final tests is shown in Figure 8.9.

The high temperature anode described was operated at full hydrogen flow (0.705 liters/minute) and at diminishing argon flow (0.27 to 0.0 liters/minute) until a pure hydrogen plasma was established. Data of thermal balance on the reactor is shown in Table 8.4. The maximum energy available downstream of the anode to effect the methane reaction was 15.3% versus the desired 35%. Visual examination of the anode at 100% H_2 flow showed that the tungsten insert was approaching maximum allowable operating temperatures. Some melt was observed around the orifice (Figure 8.8) after shutdown. No loss of material due to surface melt was observed. It is concluded that the limit of anode performance capable of long term operation without physical failure has been reached. This conclusion allows for some surface anode melt to exist during operation. Also, the melt observed was on the cathode side of the anode orifice.

At 100% hydrogen flow, 15.3% of the total energy (3.22 KW) into the reactor, representing 1685 BTU/HR, was available downstream of the anode for the methane reaction. This amounted to 495 watts or 50% more energy into the downstream hydrogen than projected necessary to accomplish the 4-man methane reaction.

Unfortunately, program termination at this point precluded testing under these conditions with methane feed into the hot gas.

Table 8.4: PLASMA THERMAL BALANCE DATA
High Temperature Anode, 0.13-inch Web

Gas Flow (L/min)		Energy Output (btu/hr)						
H_2	A	Cathode	Cathode Head*	First Constrictor Section	Anode	Second Constrictor Section	Heat Exchanger	Total
0.705	0.27	1040	275	1478	4440	975	74	8282
0.705	0.13	838	230	1815	4775	1167	31	8856
0.705	0.03	838	263	2345	5535	1635	31	10647
0.705	0.0	812 (7.4%)	275 (2.5%)	2620 (23.8%)	5600 (51.0%)	1654 (15.0%)	31 (o.3%)	10992 (100%)

*Active cooling line added to Cathode Head, part -2, Figure 4.1

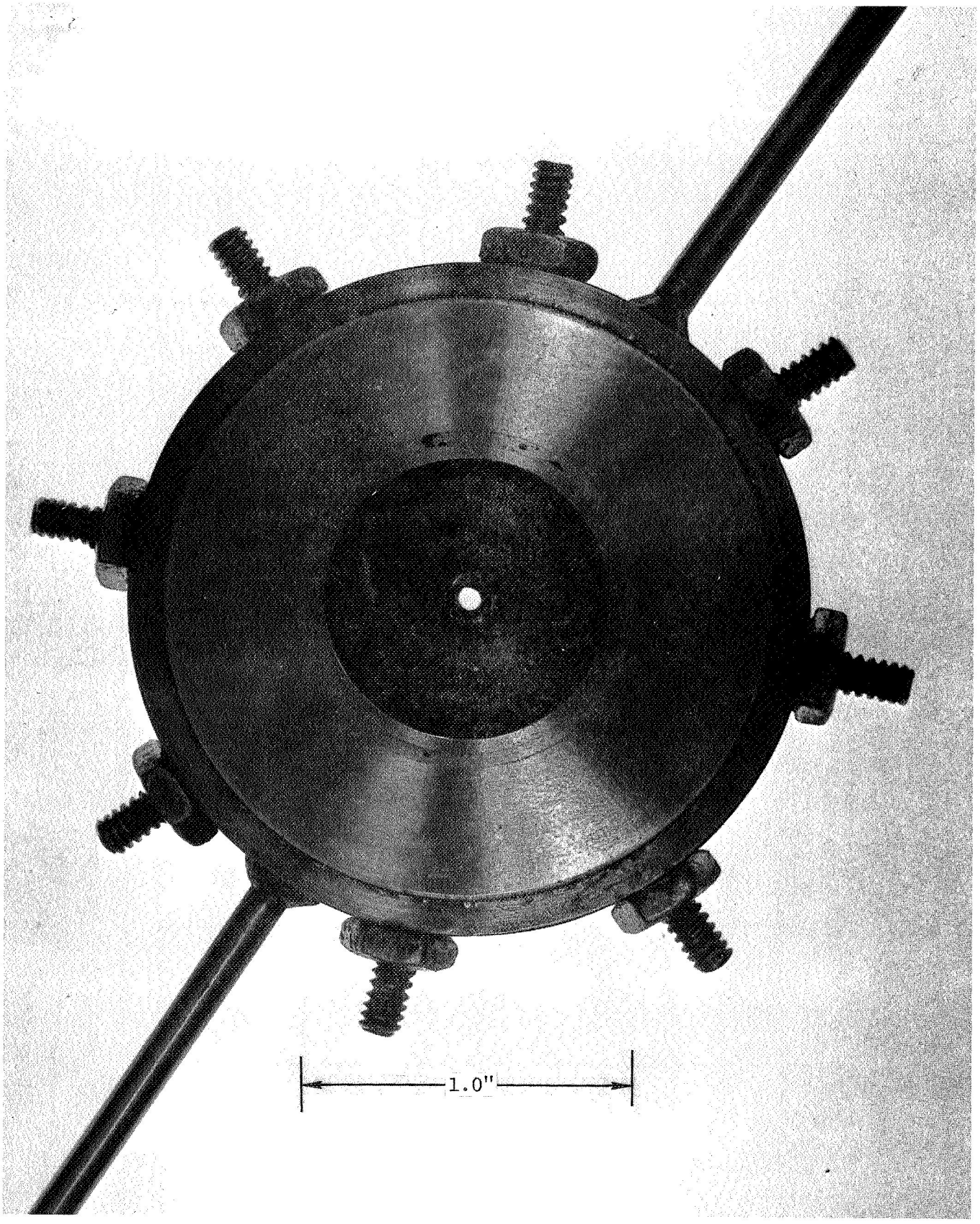

Figure 8.8: HIGH TEMPERATURE ANODE (0.13 Inches Web Thickness)

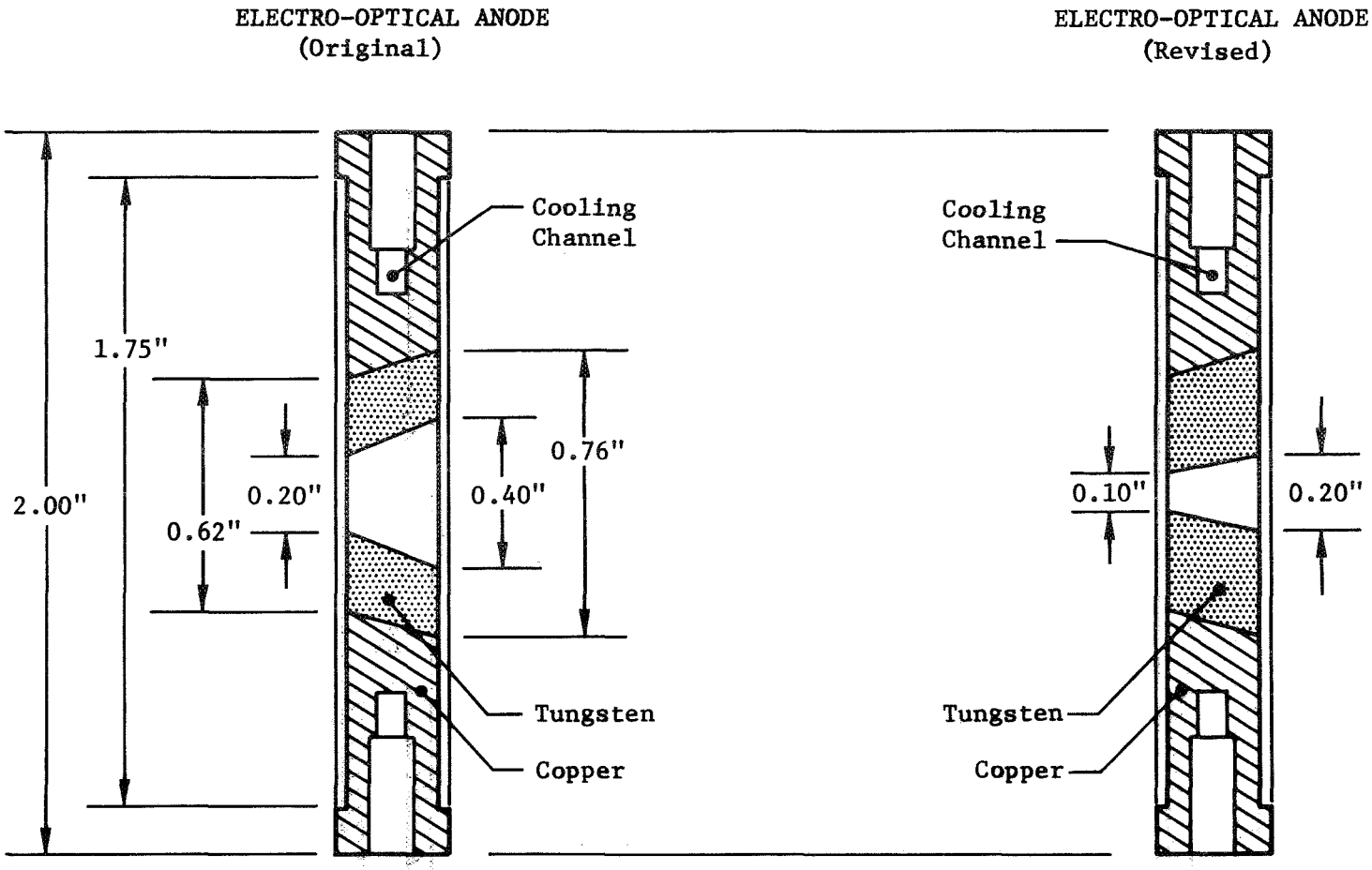

Figure 8.9A: TEST ANODE CONFIGURATIONS

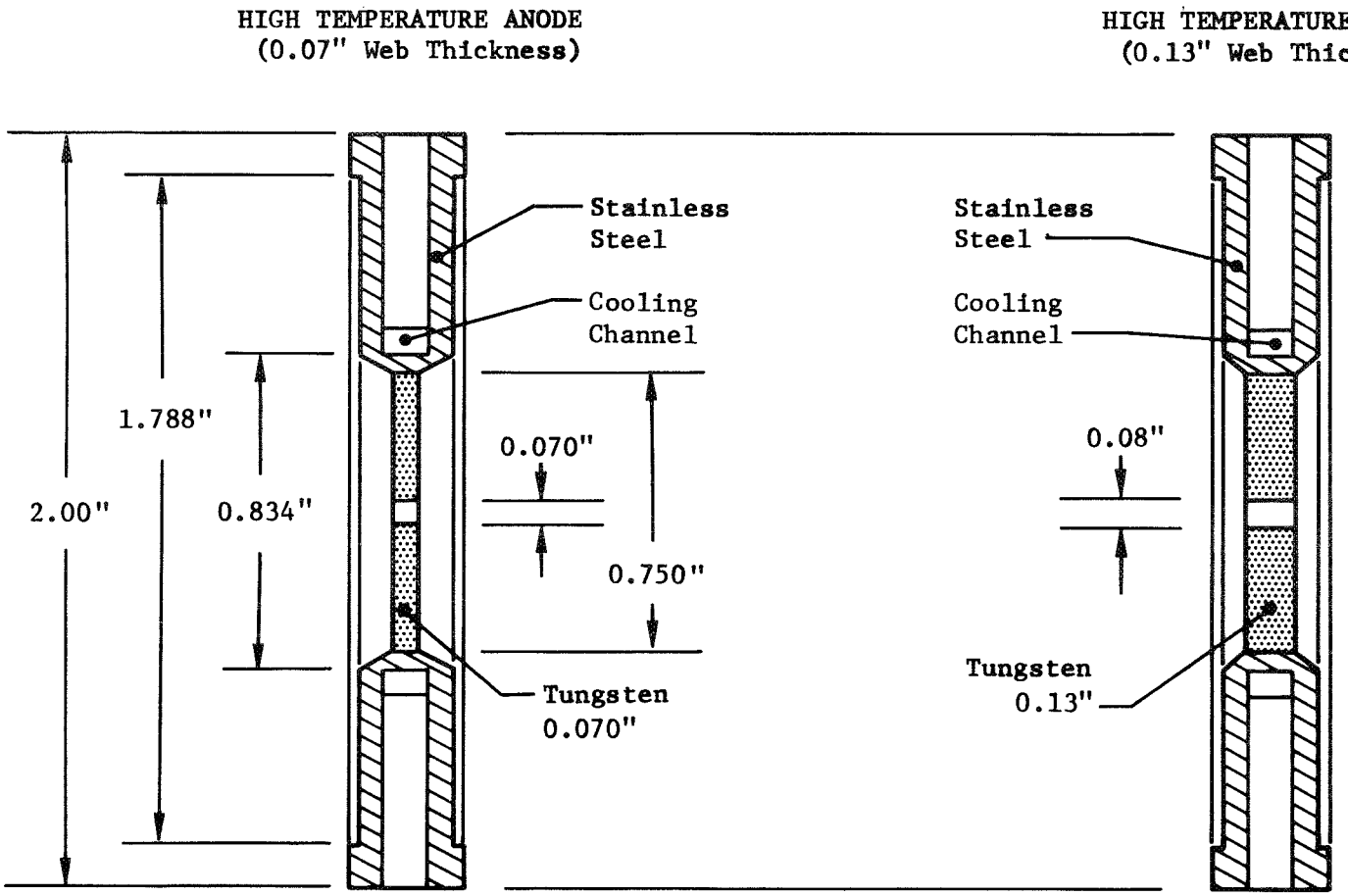

Figure 8.9B: TEST ANODE CONFIGURATIONS

9.0 SUMMARY OF RESULTS

In general, the major objective of the program was supplanted by a difficult anode development problem. Although a final anode configuration was found to produce a downstream reactant plasma, the tests necessary to determine methane-to-acetylene reaction parameters for eventual reactor design were not run as the program was terminated.

9.1 SABATIER REACTORS

The Sabatier reactors performed as predicted at the 30% excess hydrogen feed rate. They could be made to produce higher CO_2 conversion efficiencies at stoichiometric or lower hydrogen excess percentages by increasing catalyst volume (reducing space velocity). This was not necessary for this program. Adjustment of insulation for the 4 man to 9 man operating flow rates provided an effective means of proving that passive thermal control of Sabatier reactors is practical.

9.2 PLASMA REACTOR

The design and operation of hydrogen plasma arc heaters in the low flow/power regime constituted in the program is still more of an art than science. It is very apparent that the proper combination of cathode-anode geometry, power supply characteristics and anode thermal and physical design and construction techniques are extremely sensitive as small physical percentage changes create large operating variations.

After establishing the fact that a pure hydrogen plasma could be made stable at 55-60 ampere current settings, and that the cathode-anode fall voltages are significantly increased under conditions of higher currents, serious doubt as to electrical efficiency arises in the system if it is held to a 4-9 man size. A larger system (7 KW, 25 man) would operate at the same current level and at a much higher voltage level. This would tend to keep the electrical and thermal losses near that evidenced in the 3 KW system studied, thereby delivering more electrical energy into the hydrogen gas for the methane reaction.

The small geometry high energy density system as worked on in the program could be considered as reaching the limits in efficiency for scaled down hydrogen plasma arc heaters.

The final high temperature anode configuration test produced a downstream plasma equivalent to a six man system requirement. The natural next step would be to test the reactor both at higher hydrogen flow (Equivalent to six man flow requirements) and/or to feed methane to the reactor at a six man equivalent flow to establish methane reaction and hydrogen quench parameters.